geosciences

MDPI

Review

Petroleum Systems of the Shu-Sarysu Basin, Kazakhstan: A Review of Devonian–Permian Gas Potential

Almas Zhumagulov [1,2,*], Auez Abetov [3], Mehrdad T. Manzari [4] and Jamilyam Ismailova [5]

[1] International Center for Deposit Analysis and Development, Satbayev University, Almaty 050013, Kazakhstan
[2] Department of Chemical Processes and Industrial Ecology, Satbayev University, Almaty 050013, Kazakhstan
[3] Department of Geophysics and Seismology, Satbayev University, Almaty 050013, Kazakhstan; a.abetov@satbayev.university
[4] School of Mechanical Engineering, Sharif University of Technology, Tehran 111559567, Iran; mtmanzari@sharif.edu
[5] Department of Petroleum Engineering, Satbayev University, Almaty 050013, Kazakhstan; j.ismailova@satbayev.university
* Correspondence: a.zhumagulov@satbayev.university

Abstract: The Shu-Sarysu Basin in central-southern Kazakhstan remains one of the underexplored gas-prone provinces, with 12 discovered gas fields including Amangeldy (884 Bcf) and Pridorozhnoye (225 Bcf). In the context of global energy transition, such basins require integrated geological assessment to constrain exploration potential. Historical studies within the region were spatially limited and prematurely discontinued, resulting in fragmented datasets and a lack of modern interpretation. This review reassesses published geological data within a petroleum systems framework, applying contemporary geodynamic and stratigraphic concepts. Analysis shows that tectonostratigraphic evolution of the basin during Devonian–Permian time (390–250 Ma) favored formation of mature, gas-prone systems within structurally compartmentalized troughs, with effective source, reservoir, and seal configurations. Building on these findings, a three-tier classification of exploration zones is proposed based on system maturity, trap integrity, and gas shows, reflecting geological success probability. This provides a basis for prioritizing future exploration despite limited seismic and drilling coverage in many areas. Recommended priorities include digitization of archival data, structural modeling, modern geochemical and diagenetic analysis, and focused evaluation of promising areas to support future exploration.

Keywords: Shu-Sarysu Basin; Kazakhstan; Devonian–Permian succession; petroleum systems; gas prospectivity; geological evolution; stratigraphy and tectonics; energy transition

check for updates

Academic Editor: Angelos G. Maravelis

Received: 12 May 2025
Revised: 11 June 2025
Accepted: 12 June 2025
Published: 18 June 2025

Citation: Zhumagulov, A.; Abetov, A.; Manzari, M.T.; Ismailova, J. Petroleum Systems of the Shu-Sarysu Basin, Kazakhstan: A Review of Devonian–Permian Gas Potential. *Geosciences* **2025**, *15*, 232. https://doi.org/10.3390/geosciences15060232

Copyright: © 2025 by the authors. Licensee MDPI, Basel, Switzerland. This article is an open access article distributed under the terms and conditions of the Creative Commons Attribution (CC BY) license (https://creativecommons.org/licenses/by/4.0/).

1. Introduction

The global shift toward low-carbon energy increases the importance of transitional fuels. Natural gas, with its lower carbon footprint, plays a key role in energy security. Consequently, revisiting sedimentary basins with proven yet underexplored gas potential becomes increasingly relevant for bridging current energy gaps while supporting decarbonization goals. One such example is the Shu-Sarysu Basin (SSB), a sedimentary basin initiated in the Early Devonian, located in central and southern Kazakhstan (Figure 1). Building on a well-documented but regionally incomplete exploration legacy, the basin represents a suitable case for renewed system-scale evaluation, particularly within its Devonian–Permian Succession (DPS), which encompasses source, reservoir, and seal intervals, exhibits confirmed gas occurrences but remains underexplored.

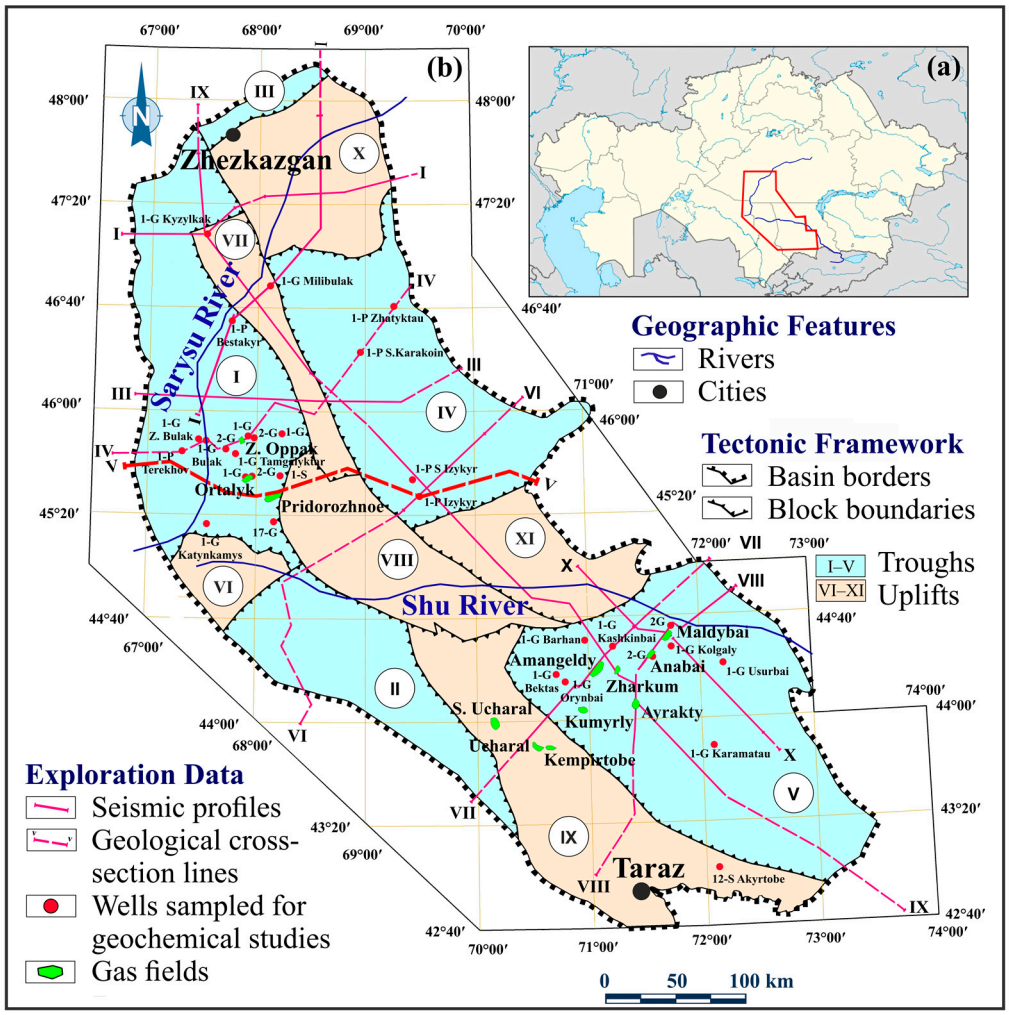


Figure 1. Location of the (**a**) Shu-Sarysu Basin (SSB) within Kazakhstan; (**b**) tectonic structure and exploration framework of the basin (modified after [1]). **Geographic features:** red frame (**panel a**)—location of the Shu-Sarysu Basin within Kazakhstan; blue solid lines—rivers; black circles—cities. **Tectonic framework:** black solid lines with square barbs—basin borders; black solid lines with barbs—tectonic block boundaries; light blue fill—troughs: I—Kokpansor Trough; II—Sozak-Baikadam Trough; III—Zhezkazgan Trough; IV—Tasbulak Trough; V—Moiynkum Trough; light brown fill—Uplifts: VI—Bugudzhil Uplift; VII—Betpakdala Uplift; VIII—Tasty Uplift; IX—Talas Uplift; X—Sarysu Uplift; XI—Lower Shu Uplift; **exploration data:** red solid lines—seismic profiles; red dashed lines—geological cross-section lines; red circles—wells sampled for geochemical studies; green polygons—gas fields.

Shu-Sarysu Basin is a composite intracontinental basin located at the junction of cratonic and orogenic domains of southern Kazakhstan. It comprises a thick Paleozoic succession including carbonate–clastic reservoirs, regional seals, and source rocks, distributed across multiple structural troughs and uplifts. Early concepts of hydrocarbon (HC) potential in the SSB emerged in the 1920s-1930s from works by Soviet geologists including Arkhangelsky, Kassin, and Satpayev [2–4]. Systematic exploration began in 1954, employing gravimetric, aeromagnetic, satellite, and seismic methods, including early common depth point profiling and later high-resolution 2D surveys [5–17]. In 1962, industrial gas inflow was recorded at the Ucharal structure (23-G), confirming prospectivity of Paleozoic succession [14]. Twelve gas fields were discovered across Talas Uplift, Moiynkum, and Kokpansor troughs. The largest accumulation, Amangeldy (884 Bcf), is primarily hosted in Late Devonian–Early Carboniferous carbonates and Early Permian clastics. Pridorozhnoye, with estimated reserves of 225 Bcf, is another major field, with hydrocarbons

trapped in terrigenous sub-salt deposits of the upper Famennian (Late Devonian) and in carbonates of the upper Visean (Early Carboniferous). Several fields also contain gas condensate [18]. Alongside drilling efforts, geochemical investigations in the 1960s–1970s focused on the Moiynkum Trough, applying luminescence-bitumen analysis and total organic carbon (TOC) measurements to assess source rock potential of Late Devonian to Carboniferous strata.

Following the discovery of oil accumulations in the South Turgay Basin in the mid-1980s, exploration efforts in the SSB were gradually scaled back as seismic acquisition capacity was redirected to regions that are more active. By the early 1990s, exploration activity had effectively come to a halt. A new phase commenced in 2001 with the issuance of exploration and development licenses to Amangeldy Gas LLP, marking the onset of pilot operations and subsequent transition to commercial production at several fields. Since 2015, high-resolution 3D seismic surveys have been extensively applied to enhance subsurface imaging and improve delineation of productive intervals. Complementary geochemical investigations, including Rock-Eval pyrolysis performed by ExxonMobil's research center (USA) on more than 400 samples across the basin, further confirmed the thermal maturity of Paleozoic formations and their potential as gas-prone source rocks [14].

Over the course of exploration and development, various basin-scale geoscientific programs were conducted by several research institutes, including KazMunayGas and the Institute of Geology and Development of Fossil Fuels. These initiatives supported a generation of predictive HC prospectivity maps and the publication of regional monographs synthesizing an evolving geological understanding of the SSB [5,6,12,19–26].

However, despite extensive historical efforts, no new discoveries have been made in the SSB since the 1980s. This exploration stagnation reflects the incompleteness of Soviet-era programs and the fragmented nature of post-Soviet investigations, resulting in uneven geological coverage across the basin. Key limitations include insufficient assessment of source rock distribution and maturity, as well as poor structural imaging in vast underexplored zones. In terms of data availability, the region includes moderately surveyed zones, primarily areas with known accumulations and vast underexplored tracts where only indirect HC indications have been recorded. Exploration activities remain limited to the reconnaissance stage. In many sectors, drilling density does not exceed two wells per 1000 km^2, and seismic coverage remains below 13 km per 100 km^2, indicating extremely low resolution. Most legacy data are outdated and exist only in analog formats, posing challenges for integration into modern digital workflows. In addition, published scientific assessments present inconsistent interpretations of system maturity and functionality, underscoring the need for a basin-wide re-evaluation of HC potential.

In response to existing challenges, this study applies a petroleum system analysis framework [27] to evaluate gas prospectivity within underexplored regions of the DPS in the SSB, focusing on the spatiotemporal evolution and functional integrity of system elements. This methodological approach is consistent with petroleum system studies that apply similar integrative frameworks to evaluate geological success in underexplored basins. Prior works emphasize functionality-based assessments of key system elements, including source, reservoir, seal, trap configuration, and migration pathways, as indicators of exploration prospectivity [28]. To achieve this, the study addresses the reconstruction of spatiotemporal evolution of Devonian–Permian petroleum systems in a geological context (1), and the evaluation of system functionality through assessment of maturity, integrity, and effectiveness of key elements, and the identification of possible subsurface hydrocarbon migration pathways (2). Results are interpreted to delineate prospective zones for gas generation and accumulation and to guide prioritization of future exploration. This approach enables the systematization of existing geological datasets and reassessment of current

knowledge on the DPS (1), as well as refinement of the conceptual model of petroleum system formation (2). It also supports the evaluation of present-day maturity, continuity, and effectiveness of petroleum systems (3), the identification of prospective zones within poorly studied areas (4), and the definition of directions for reducing geological uncertainty and improving exploration coverage in data-deficient regions (5).

2. Reconstruction of the Spatiotemporal Evolution of Devonian–Permian Petroleum Systems in the Geological Context

This section aims to reconstruct geological conditions that shaped the configuration of petroleum systems in the SSB, based on analysis of the lithostratigraphic framework and the spatiotemporal evolution of Devonian–Permian systems in the geological context. Some of the regional tectonic interpretations and lithostratigraphic correlations presented here were originally reported in Soviet-era geological surveys, while others reflect reinterpretations based on more recent structural syntheses and geochronological data.

The non-marine SSB lies within the Central Asian Orogenic Belt (Altaids), formed during a series of Paleozoic orogenic events spanning from the early Cambrian to the late Carboniferous [28,29]. It extends approximately 840 km NW-SE and 300 km across, covering an area of about 160,000 km^2. Chu-Ili Range, a system of low-relief mountains trending NW-SE, forms the eastern boundary of the SSB. In the north, Sarysu-Teniz watershed separates it from the Teniz Basin, while the Ulytau Range marks the northwestern margin adjoining the Turgay Basin. To the southwest, Karatau Ranges divide it from the Karatau-Syrdarya Basin, and the Kyrgyz-Terskey Range (Figure 2) bound the southern limit, representing orogenic features closed during late Paleozoic time, which framed the subsequent subsidence of the SSB [14,28].

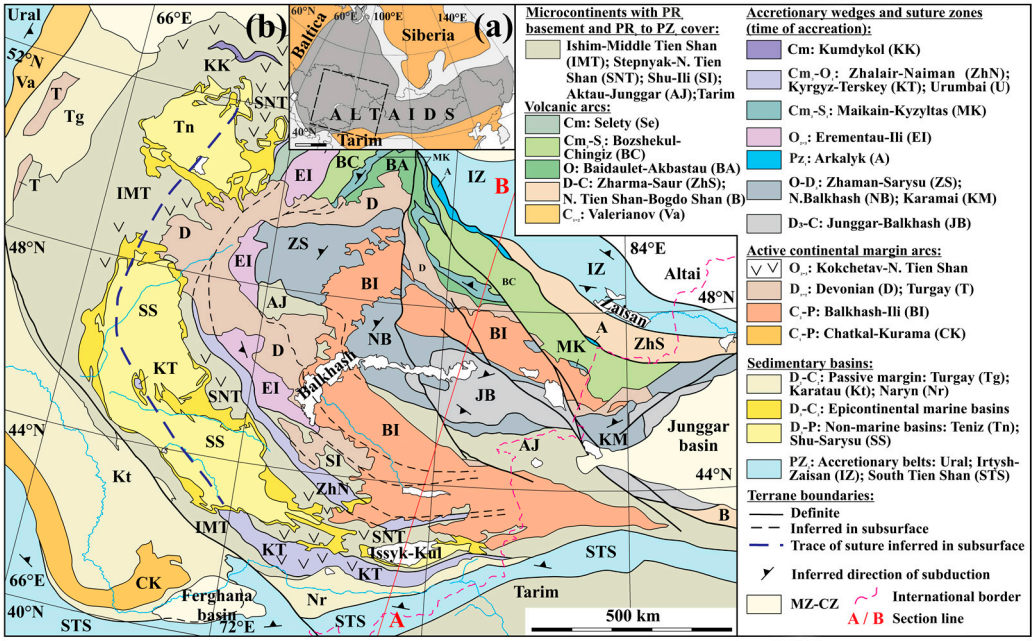


Figure 2. Simplified geotectonic map of the (**a**) Central Asian Orogenic Belt; and (**b**) Kazakhstan Orocline (modified after [29]). **Microcontinents with PR$_1$ basement and PR$_2$ to PZ$_1$ cover:** IMT—Ishim–Middle Tien Shan; SNT—Stepnyak–North Tien Shan; SI—Shu-Ili; AJ—Aktau-Junggar; Tarim—Tarim. **Volcanic arcs:** Se—Selety (Cm); BC—Bozshekul-Chingiz (Cm$_2$-S$_1$); BA—Baidaulet-Akbastau (O); ZhS—Zharma-Saur (D-C); B—North Tien Shan-Bogdo Shan (D-C); Va—Valerianov (C$_{1\text{-}2}$). **Accretionary wedges and suture zones:** KK—Kumdykol (Cm); ZhN—Zhalair-Naiman (Cm$_3$-O$_1$); KT—Kyrgyz-Terskey (Cm$_3$-O$_1$); U—Urumbai (Cm$_3$-O$_1$); MK—Maikain-Kyzyltas (Cm$_2$-S$_1$); EI—Erementau-Ili (O$_{2\text{-}3}$); A—Arkalyk (Pz$_1$); ZS—Zhaman-Sarysu (O-D$_3$); NB—North Balkhash (O-D$_3$);

KM—Karamai (O-D_3); JB—Junggar-Balkhash (D_3-C). **Active continental margin arcs:** VV—Kokchetav-North Tien Shan (O_{2-3}); D—Devonian arc (D_{1-2}); T—Turgay arc; BI—Balkhash-Ili (C_2-P); CK—Chatkal-Kurama (C_1-P). **Sedimentary basins:** light pink fill—passive margin (D_2-C_2): Tg—Turgay; Kt—Karatau; Nr—Naryn; yellow fill—epicontinental marine basins (D_3-C_2); light yellow fill—non-marine basins (D_3-P): Tn—Teniz; SS—Shu-Sarysu; light blue fill—accretionary and collisional belts (PZ_3): Ural—Ural; IZ—Irtysh-Zaisan; STS—South Tien Shan. **Terrane boundaries:** solid black line—definite; dashed line—inferred in subsurface; blue dashed line—trace of suture inferred in subsurface; black triangle line—inferred direction of subduction; white fill—MZ-CZ; pink dashed line—international border; solid red line—A/B section line.

2.1. Lithostratigraphic Framework

Lithostratigraphic structure of the SSB reflects its position within a tectonically active domain of the Caledonian structural belt in southwestern Central Kazakhstan and northern Tien Shan [14]. This setting, shaped by evolution of the adjacent Dzhungar-Balkhash geosyncline during the early Paleozoic to early Carboniferous, promoted basement mobility and fragmentation into large fault-bounded blocks. Differential displacement along these blocks led to structural deformation of pre-Jurassic strata and influenced present-day configuration of the basin (Figure 3) [29–42].

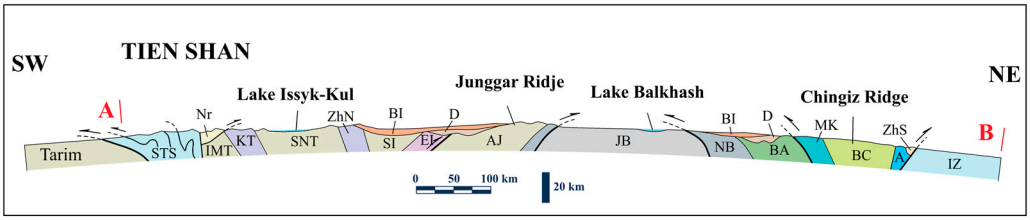


Figure 3. Schematic cross-section across Kazakhstan Orocline from the Tarim Basin to the Altai, along line A–B, indicated in Figure 2. Vertical exaggeration: 1:2 (modified after [29]). Arrows—tectonic movement directions; other abbreviations are as in Figure 2.

Regionally, lithostratigraphic architecture of the SSB, spanning from the Devonian to the Cenozoic, appears relatively consistent, with local variations in thickness reflecting structural segmentation. Sedimentary fill in the SSB exceeds 5500 m in thickness. Crystalline basement comprises Precambrian and Paleozoic (Cambrian to Carboniferous) metamorphosed volcanic and sedimentary formations, characterized by block structure and widespread surface exposure along basin margins and intrabasin uplifts (Figures 1 and 3). It is unconformably overlain by a thick DPS, including Devonian carbonate, clastic, and evaporite assemblages; Carboniferous clastic-carbonate units and continental red beds; and Permian clastic-evaporite and clastic-carbonate successions. These overlying successions accumulated during and after the Hercynian (Variscan) orogenic phase, which shaped the regional structural configuration in late Paleozoic time. Overlying these are Mesozoic–Cenozoic sediments, up to 300 m thick, which rest unconformably and occur as nearly flat-lying layers composing the uppermost part of basin fill (Figure 4) [9,31–37,40–45].

2.2. Spatiotemporal Evolution of Devonian-Permian Petroleum Systems in the Geological Context

The SSB evolved through five main tectonic stages: Early to Middle Devonian extensional regime (1); Late Devonian to Early Carboniferous passive margin development (2); and Middle Carboniferous to Late Permian convergence and regional uplift (3). These were followed by Triassic to Early Jurassic compressional inversion (4), and Early Jurassic to Early Pliocene sagging, with Late Pliocene Himalayan-related compression (5) (Table 1) [29,38,46–79].

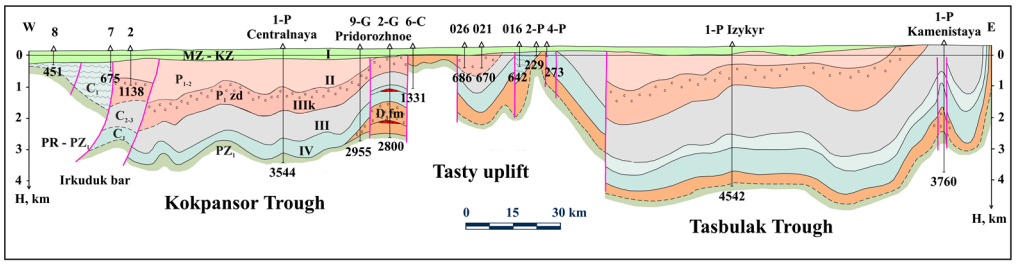


Figure 4. Geological section along V–V line (see Figure 1) illustrating lithostratigraphic framework of Kokpansor Trough, Tasty Uplift, and Tasbulak Trough (modified after [1]). PR—Proterozoic; green fill (PZ_1)—Early Paleozoic; orange fill (D_3fm)—Famennian (Late Devonian) evaporitic succession; light green fill (C_1)—Early Carboniferous; light grey (C_{2-3})—Middle to Late Carboniferous; pink (P_1zd)—Zhidelisai (Early Permian) evaporitic succession; light pink (P_{1-2})—Early to Late Permian; very light green (MZ-KZ)—Mesozoic–Cenozoic cover; I—IV—marker horizons; H—depth; 1P, 2G, etc.—exploration wells; pink vertical lines—faults; dashed lines—inferred boundaries of tectonostratigraphic units; cc—evaporitic horizons; wavy lines—metamorphic rocks.

Table 1. Tectonic evolution stages of the Shu-Sarysu Basin [28,29].

Stage	Time Period	Tectonic Setting/Key Processes
1	Early to Middle Devonian	Back-arc rifting, arc volcanism, alluvial-volcanic deposition; evaporite accumulation in restricted lagoons during platform transition.
2	Late Devonian to Early Carboniferous	Transition to passive margin; major marine transgression; development of evaporitic and carbonate depositional systems.
3	Middle Carboniferous to Late Permian	Tectonic compression, collision, and uplift; block faulting and development of lacustrine and alluvial plains under arid conditions.
4	Triassic to Early Jurassic	Collision-related inversion and uplift (Eocimmerian tectonic phase), due to compressional reactivation of earlier extensional structures.
5	Early Jurassic to Present	Post-orogenic basin sagging (Early Jurassic–Early Pliocene), followed by Himalayan compression and fault reactivation (since Late Pliocene).

This long-lived tectonic evolution was preceded by the amalgamation of Proterozoic–Paleozoic microcontinents and island arcs into the Kazakhstan continent, largely completed by Late Ordovician–Early Silurian. The SSB formed as part of this composite landmass, whose emergence coincided with Caledonian orogeny [39,57,60]. The resulting topography was highly dissected, with the development of northwest-trending deep faults segmenting the crystalline basement [41,59,64,65]. These tectonic stages critically influenced the spatial architecture of the basin and controlled the distribution of key petroleum system elements. Rift-related subsidence and passive margin development favored the widespread deposition of potential source rocks and carbonate reservoirs, while compressional and inversion phases facilitated trap formation and structural compartmentalization [46]. However, the reconstruction of basin-wide tectonostratigraphic controls is partially based on generalization from selected well-characterized troughs. Structural and sedimentary interpretations for peripheral or deeply buried segments rely on regional extrapolation and published syntheses, as high-resolution subsurface data are not uniformly available across the basin.

2.2.1. Devonian: Extensional Tectonics and Evaporite Deposition

Initial subsidence of the SSB began during Early to Middle Devonian in an extensional tectonic setting, likely influenced by subduction-related dynamics along southeastern margin of the Kazakhstan continent, then located at southern latitudes of the Northern Hemisphere (0–30° N) (Figure 5) [42,52,80–85]. Subduction of Junggar-Balkhash oceanic plate beneath the continental margin initiated formation of an Andean-type volcanic arc and development of the Devonian volcanic belt of Central Kazakhstan [43,67,68,74,82,86]. Rift-

related back-arc and foreland basins, including Shu-Sarysu and Teniz, accumulated volcanic and alluvial material within actively subsiding troughs [46,84–87]. By Frasnian, tectonic activity waned and transition to a platform regime occurred. Spreading in surrounding oceanic domains ceased, and a major transgression advanced from the northeast during Famennian to Early Carboniferous time during the early phase of the Hercynian (Variscan) orogeny, which progressively influenced basin architecture and sedimentation [48–50,84,85]. The Shu-Sarysu region evolved into a low-relief accumulation plain under conditions of arid climate, elevated temperatures, and tectonic stability. Two periodically connected hypersaline lagoons developed, depositing three evaporite cycles separated by carbonate–clastic units [51,84]. Late Devonian faulting associated with Hercynian orogeny overprinted earlier northwest-trending structures, resulting in basement block fragmentation and the onset of block tectonics [53,84,87]. These evaporite-rich successions established early regional seal potential, while restricted marine inflow limited widespread source rock development [54,58,83,87]. The extensional setting, associated with localized subsidence, created accommodation space for organic-rich sediments, while evaporite precipitation under restricted conditions led to the formation of regionally effective sealing facies.

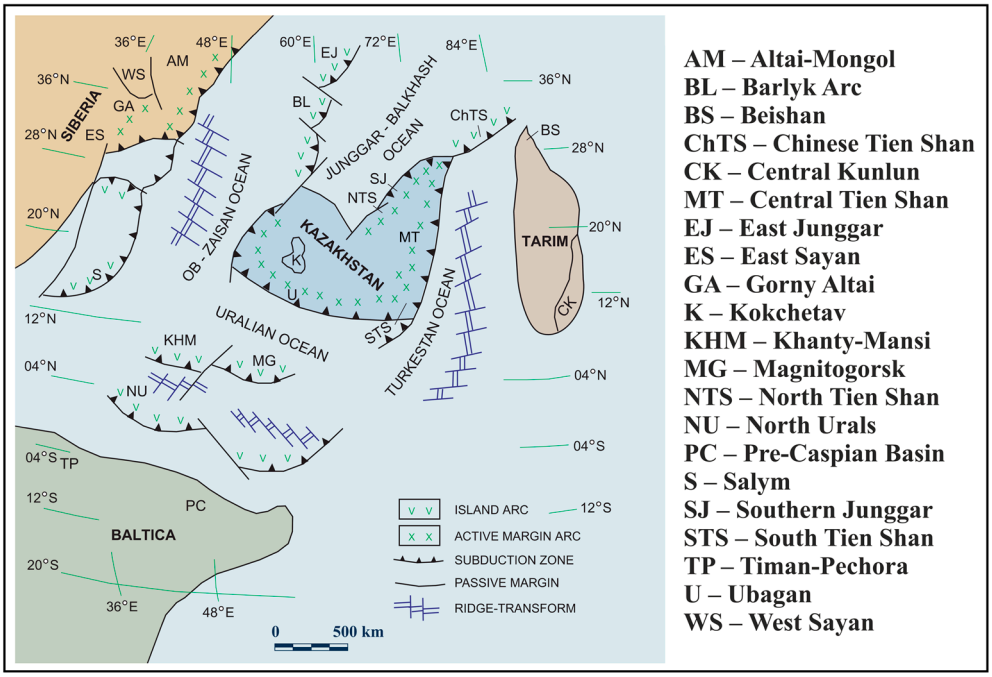


Figure 5. Palinspastic map showing the tectonic configuration of the Central Asian Orogenic Belt during the Early Devonian, 390 Ma (modified after [29]). AM—Altai-Mongol; BL—Barlyk Arc; BS—Beishan; ChTS—Chinese Tien Shan; CK—Central Kunlun; MT—Central Tien Shan; EJ—East Junggar; ES—East Sayan; GA—Gorny Altai; K—Kokchetav; KHM—Khanty-Mansi; MG—Magnitogorsk; NTS—North Tien Shan; NU—North Urals; PC—Pre-Caspian Basin; S—Salym; SJ—Southern Junggar; STS—South Tien Shan; TP—Timan-Pechora; U—Ubagan; WS—West Sayan; VV—Island arc; ××—Active margin arc; Sawtooth line—Subduction zone; Wavy line—Passive margin; Double-bar line—Ridge-transform boundary.

2.2.2. Carboniferous: Marine Transgression and Carbonate Platform Development

Following Late Devonian evaporite deposition and initiation of extensional block tectonics, Carboniferous sedimentation marked a shift toward widespread marine transgression and the development of carbonate platforms across the basin [54,55]. During Tournaisian and early Visean, marine transgression reached the maximum extent. Thick dolomitized limestones accumulated along northern and eastern basin margins through chemical sedimentation. Continued transgression under humid climatic conditions in

late Tournaisian–early Visean facilitated the widespread deposition of dark-colored clay–carbonate facies rich in organic matter, derived from swampy plains of Moiynkum Trough and adjacent blocks. By middle Visean, sea level stabilized, terrigenous input diminished, and carbonate sedimentation became dominant. Numerous bioherms and carbonate platforms developed across the basin. These carbonate buildups served as potential reservoir facies, often overlain by fine-grained clastics, creating vertical juxtaposition favorable for hydrocarbon entrapment. Diagenetic transformations also began to operate during burial and early lithification stages, progressively altering the petrophysical properties of reservoir and seal rocks. These processes, such as cementation, dissolution, and mineral transformation, set the foundation for later hydrocarbon generation and entrapment conditions [43]. Toward the end of Visean, renewed shallowing reintroduced terrigenous influx [56,66]. During Serpukhovian, transition from marine to subaerial settings occurred. Unified epicontinental sea fragmented, and Sarysu-Teniz watershed formed [58,61–63]. Organogenic-detrital limestones were replaced by clastic infill in subsiding troughs.

From Late Serpukhovian to Middle Carboniferous, renewed subduction along margins of the Kazakhstan continent triggered widespread compression. Volcanic belts developed along active convergent boundaries, while collisional interaction intensified with Baltica, Siberian, and Tarim blocks, culminating in the closure of peripheral oceanic domains. During Late Carboniferous, the basin was dominated by extensive alluvial-lacustrine plains [52,67,68]. Red-colored claystones, interbedded with siltstones and subordinate limestones, accumulated under increasingly arid conditions. Isolated lakes periodically coalesced into larger water bodies during wetter intervals. This evolution supported the development of oil-prone source rocks in Early Carboniferous under anoxic conditions, carbonate reservoirs during sea-level highstands, and gas-prone continental clastics in Late Carboniferous successions [28,76]. The interplay between marine transgression, anoxic conditions, and tectonic quiescence promoted the widespread development of oil-prone source rocks, while subsequent continental deposition during compressional phases enhanced gas-prone potential and structural complexity conducive to trap formation.

2.2.3. Permian: Structural Segmentation and Lacustrine Evaporitic Systems

These Late Carboniferous depositional regimes gradually evolved under continued extensional tectonic differentiation and increasing aridification, setting the stage for structural segmentation and evaporitic basin development during the Permian [69,77]. Permian tectonics were marked by the major reorganization of the regional structural framework as the Kazakhstan continent amalgamated with Siberian, Baikal, and Tarim platforms. This consolidation finalized the assembly of Eurasian landmass and established the modern structural architecture of Central Kazakhstan. Within the SSB, differential block movement resulted in segmentation into actively subsiding troughs (Kokpansor, Moiynkum, Sozak-Baikadam, Zhezkazgan, Tasbulak) and intervening uplifts (Sarysu, Lower Shu, Betpakdala, Tasty, Talas, Bugudzhil) [49,70,71]. During Early Permian, large lacustrine systems persisted in basin interior, where sandy-silty deposits transitioned into carbonate–sulfate assemblages under intensifying arid conditions. By Late Permian, distinct hydrochemical regimes developed: the northern sub-basin evolved into a hypersaline setting, while the southern sub-basin maintained near-normal salinity. Widespread accumulation of variegated mudstones, siltstones, and marl interbeds occurred under these conditions. The resulting depositional systems promoted evaporite seal formation and localized heterogeneity in potential reservoir facies, particularly within central depocenters [69]. Differential tectonic subsidence and evolving depositional regimes during the Permian led to pronounced heterogeneity in reservoir quality and seal continuity. Evaporitic and carbonate-rich successions accumulated preferentially in structurally confined depocenters, enhancing vertical

seal efficiency and lateral facies variability within potential reservoir units. While these trends are supported by facies analysis in well-studied troughs, their continuity and exact spatial extent in underexplored sectors remain uncertain due to sparse well control and limited seismic imaging.

2.2.4. Mesozoic and Cenozoic: Post-Paleozoic Modifications (Contextual Overview)

While Permian tectonics largely defined the structural and facies framework of the basin, subsequent Mesozoic and Cenozoic events introduced additional modifications restricted to near-surface levels. Although not a primary focus of this study, Mesozoic and Cenozoic intervals were characterized by successive tectonic overprints and erosion phases. During Triassic and Jurassic, uplift and faulting reshaped basin margins, accompanied by surface denudation and weathering. These processes likely reflect the regional effects of Eocimmerian tectonic activity, which resulted in non-deposition and erosion across much of the basin. From Eocene to Oligocene, shallow marine conditions briefly returned, followed by continental sedimentation during Neogene–Quaternary. Major fault reactivation (e.g., Karatau and North Kyrgyz faults) in Late Cenozoic triggered renewed subsidence in the Sozak-Baikadam Trough, leading to deposition of molasse-type clastics [61]. These events predominantly influenced upper stratigraphic levels and surface morphology, with no documented disruption of deeper DPS [78,88,89].

3. Functional Analysis of Devonian–Permian Petroleum Systems Focused on the Maturity, Integrity, and Effectiveness of Their Key Elements

This section evaluates the present-day functional state of Devonian–Permian petroleum systems in SSB through analysis of maturity, integrity, and interaction efficiency among key system elements.

3.1. Source Rocks and Thermal Maturity

Assessment of source rocks in the SSB encompasses both legacy Soviet-era geochemical studies and modern investigations employing high-resolution instrumental analysis. Between 1968 and 1976, the Institute of Geology and Development of Fossil Fuels conducted initial geochemical work, including luminescence-bituminological analysis, bitumen extraction, and TOC measurements on 117 samples of claystones and carbonates [14,80,90]. The results revealed bituminous character of Early Carboniferous and Permian terrigenous and carbonate rocks, with marine-type kerogen and bitumen content reaching up to 2.25%. However, analytical techniques available at the time did not allow for quantitative assessment of thermal maturity or HC generation potential.

A breakthrough in thermal maturity and HC generation potential assessment was achieved in 2003–2004, when ExxonMobil's Houston research center conducted Rock-Eval pyrolysis on 405 samples from 29 wells (Figure 6). Thermal maturity parameters derived from Rock-Eval pyrolysis are discussed further below in the context of regional burial and geothermal history. TOC content was below 1% in most samples, with approximately 10% exceeding 1%, and only a few exceeding 2%. The Hydrogen Index (HI) was consistently below 75 mg HC/g TOC across all samples, indicating fully exhausted kerogen typical of gas-prone systems [14,28].

Production Index (PI) values derived from Rock-Eval data (Table 2) range from 0.11 to 1.00, with most mature samples exhibiting PI > 0.5. These values indicate a high level of catagenetic maturity and completion of primary oil and gas generation phases. Elevated PI values in Visean intervals of the Tasbulak and Moiynkum troughs further support the regional thermal maturity trends. This pattern is consistent with the geothermal

interpretation presented later in this section [14,28]. A more detailed interpretation of maturity gradients and their geodynamic drivers is provided below.

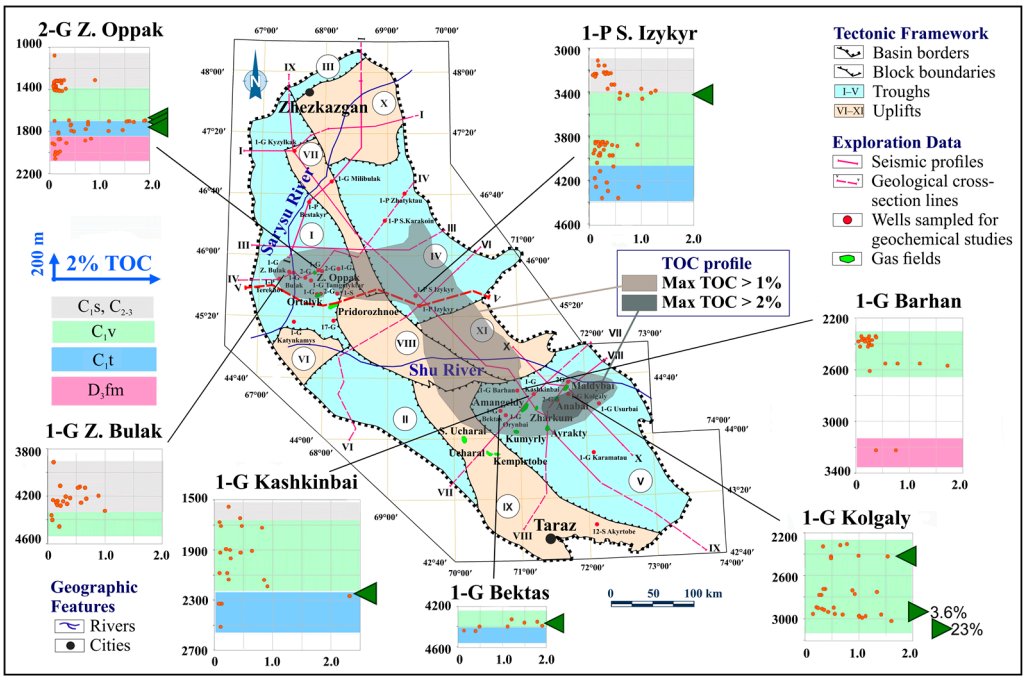


Figure 6. Locations of sampled wells and TOC profiles by depth and stratigraphy in the SSB (Rock-Eval pyrolysis) (modified after [1,14,45]). TOC—total organic carbon; light grey fill—C_1s (Serpukhovian, Early Carboniferous) to C_{2-3} (Middle–Late Carboniferous); light green fill—C_1v (Visean, Early Carboniferous); blue fill—C_1t (Tournaisian, Early Carboniferous); pink fill—D_3fm (Famennian, Late Devonian); grey shading—Intervals with TOC > 1%; dark grey shading—intervals with TOC > 2%; green triangles—sampled well intervals with maximum TOC values; orange dots—TOC measurements from representative wells; other abbreviations are as in Figure 1.

Table 2. Geochemical indicators of maturity and source rock exhaustion in the Tasbulak, Moiynkum, and Kokpansor Troughs. TOC—total organic carbon; Tmax—temperature of maximum hydrocarbon generation; Ro—vitrinite reflectance; HI—Hydrogen Index; PI—Production Index.

Parameter	Tasbulak Trough	Kokpansor Trough	Moiynkum Trough
TOC, %	0.8–1.87	0.77–1.91	0.78–1.9 (22.97)
Tmax, °C	318–379	300–532	301–579
Ro, %	1.49–3.3	1.55–2.42	1.39–3.26
HI, mg HC/g TOC	3–52	2–72	8–70
PI	0.26–0.89	0.31–0.8	0.11–1.0

The generation and preservation of source rocks in the SSB were closely governed by its tectonic and sedimentary evolution. Rift-related subsidence during the Devonian created accommodation space for lacustrine and marginal-marine organic-rich facies. Subsequent passive margin conditions and transgressions during the Carboniferous facilitated widespread deposition of coaly and carbonate–argillaceous intervals with high TOC values. Later compressional and sagging phases drove deep burial, structural segmentation, and thermal maturation, resulting in spatial heterogeneity of source rock properties across different troughs and uplifts. The highest levels of organic enrichment (1.5–6% TOC) occur in coal-bearing lacustrine–palustrine deposits of Visean age in the NE and SE parts of the basin, primarily within the Tasbulak and Moiynkum troughs, as well as on the margins of the Lower Shu Uplift. These organic-rich successions underwent deep burial and advanced catagenesis, acting as the principal gas source for fields such as Amangeldy and

Airakty. Elevated nitrogen concentrations observed in degassing products from horst-block reservoirs are most likely linked to deep thermal generation from high-rank coaly intervals subjected to elevated temperatures [90–93].

Recent studies [43,91–96] have shown that the Visean (C_1v) and Serpukhovian (C_1sr) intervals are composed of carbonates with clay admixtures. TOC values range from 0.19% to 1.91%, HI from 1.7 to 41.3 mg HC/g TOC, with Tmax around 465 °C and Ro in the range of 1.2–1.5%, consistent with thermally mature type III kerogen. Application of TOC reconstruction methods [42], using correction factors of 1.6–2.0, suggests that the original generative potential of these deposits was favorable for gas and, to a lesser extent, for condensate. A stratigraphic summary of TOC variability (Table 3) includes minimum, mean, and maximum values for each interval, reflecting the full range of organic richness across structural domains. TOCmin values as low as 0.02–0.25% characterize background conditions and organic-lean facies, while TOCmax values up to 22.97% highlight localized intervals with elevated generative potential. TOCmean values, ranging from approximately 0.2% in marls to nearly 1.9% in coaly and lacustrine facies, capture representative organic content within each depositional setting. These metrics provide a more differentiated assessment of source rock quality and facilitate comparison between tectonostratigraphic zones.

The complex catagenetic history of the SSB reflects a variable geothermal regime (Table 2). The temperature of maximum hydrocarbon generation (Tmax) reaching up to 579 °C and vitrinite reflectance (Ro) reaching 3.3% indicate a mature stage of type III humic kerogen in Late Devonian (D_3fm) and Early Carboniferous (C_1t-v_1) deposits. Particularly elevated PI values (0.78–1.00) were recorded in Visean deposits of the Moiyn-kum and Tasbulak troughs, where Tmax exceeds 470 °C, Ro is above 2%, and residual HI remains below 50. Modeling shows that the current thermal gradient (30–35 °C/km) and burial depths up to 4.5 km cannot fully explain the observed maturity levels. Such levels can only be explained by elevated paleo-geothermal gradients (4.3–4.5 °C/100 m), likely driven by tectonic pulses and deep heat flow during the Late Paleozoic, possibly associated with subduction-related magmatism and synorogenic thermal anomalies linked to the Hercynian orogeny. This interpretation is consistent with available data from central and southern troughs. However, thermal conditions in northern and marginal areas are inferred rather than directly measured, which introduces spatial uncertainty in maturity assessments across the entire basin. This transient high-heat regime, combined with a short residence time within the oil window (estimated at 3–5 million years) and rapid subsidence into the deeper catalytic gas generation zone, favored the formation of gaseous HC over liquid phases [14,83,94–97]. This interpretation is supported by the absence of confirmed oil accumulations and the limited occurrence of oil traces such as bitumen coatings, impregnations, and fluid inclusions only in isolated core intervals from deep or structurally elevated wells in the Lower Shu Uplift and northern Moiynkum Trough. These thermal maturity conditions are corroborated by mineralogical studies showing the presence of dispersed organic matter embedded in feldspar-rich terrigenous rocks, particularly in the Carboniferous–Permian section of the southwestern basin. X-ray diffraction analyses identified DOM concentrations of up to 2%, localized within microcrystalline calcite and clay matrices (e.g., montmorillonites). This configuration indicates advanced catagenetic transformation and thermal cracking potential under deep burial, aligning with gas-prone character observed across high-PI intervals [97].

Table 3. Stratigraphic and geochemical attributes of source rock intervals in key structural blocks. P_1—Early Permian; C_3-P_1—Late Carboniferous–Early Permian; C_1s—Serpukhovian (early Carboniferous); C_1v—Visean (Early Carboniferous); C_1v_1—Early Visean (Early Carboniferous); C_1—Early Carboniferous; C_1t-v_1—Tournaisian–Early Visean (Early Carboniferous); D_3fm—Famennian (Late Devonian).

Location	Age	Lithology	Thickness (m)	TOC Min (%)	TOC Mean (%)	TOC Max (%)	Kerogen Type
Zhezkazgan Trough	P_1	Bituminous marls	up to 1500	0.02	0.17	0.3	-
Tasbulak Trough	P_1	Bituminous marls	up to 600	0.07	0.22	0.3	-
Kokpansor Trough	P_1	Bituminous marls	up to 150	0.08	0.21	0.3	-
Talas Uplift	C_3–P_1	Argillites, clays, carbonates	up to 50	0.05	0.27	0.43	-
Talas Uplift	C_1s	Carbonates, marls	up to 150	0.05	0.75	2.5	Various
NE Moiynkum Trough	C_1s	Carbonates, argillites, marls	up to 150	0.25	1.33	1.9	Humic
Talas Uplift	C_1v	Carbonates, marls	up to 200	0.15	1.1	2.57	Various
NE Moiynkum Trough	C_1v	Carbonates, argillites, marls	up to 200	0.05	0.78	4.24	Humic
NE Moiynkum Trough	C_1v_1	Lacustrine–palustrine rocks, coals	up to 200	0.49	1.9	5.6/22.97	Humic
Kokpansor Trough	C_1	Carbonates, marls	up to 350	0.06	1.91	4.53	Various
SW Tasbulak Trough	C_1	Carbonates, marls	up to 350	0.08	1.87	4.53	Various
Other basin areas	C_1	Siltstones, clays, marls	up to 350	0.24	1.8	4.53	Various
Lower Shu Uplift	C_1t–v_1	Siltstones, clays	up to 200	0.38	1.8	4.24	-
Central Talas Uplift	C_1t–v_1	Siltstones, clays	up to 150	0.13	1.23	4.24	-
SE Kokpansor Trough	D_3fm	Argillites, marls	up to 150	0.15	0.77	3.49	Sapropelic
SE Tasbulak Trough	D_3fm	Clays	up to 150	0.14	0.8	1.87	Sapropelic
Lower Shu Uplift	D_3fm	Siltstones, clays	up to 150	0.08	0.9	1.75	Sapropelic

Integrated analysis of stratigraphic architecture and lithological composition (Table 3), together with thermal maturity and residual organic matter indicators (Table 2; Figure 6), reveals distinct spatial trends in source rock quality across the basin. The Kokpansor and Moiynkum troughs contain the most thermally evolved intervals, marked by high Tmax and Ro values and depleted TOC and HI, consistent with complete HC generation and expulsion.

3.2. Reservoir Rocks

Both conventional (unfractured) and naturally fractured reservoirs have been established within the DPS, ranging in age from Famennian to Early Permian.

3.2.1. Conventional Reservoirs

Conventional HC accumulations are established in red-colored and variegated sandstones of Famennian age in Kokpansor Trough, as well as in Tournaisian, early Visean, and Early Permian strata in Moiynkum Trough (Figure 7). These reservoirs exhibit both zonal and regional distribution patterns, with broader occurrences documented in other parts of the basin, and generally possess favorable petrophysical properties. Tectonic subsidence during Devonian and Early Carboniferous stages created structurally controlled depocenters that accumulated thick siliciclastic and carbonate sequences, forming the primary reservoir units. Regional transgressions and platform development favored lateral continuity of sand bodies and carbonates, while syndepositional tectonics influenced facies transitions and thickness variations. Porosity and permeability values represent typical reservoir property ranges established from core and well-log analyses. According to core and well-log analyses, porosity in Famennian sandstones ranges from 7 to 27%, with maximum permeability reaching 12 mD. In the Early Carboniferous sandstones, the values of open porosity coefficients vary from 3 to 21.6%, and permeability is generally less than 190 mD. Middle–Late Carboniferous and Early Permian sandstones have porosity values ranging from 3 to 10% and 19 to 22%, respectively, with permeability reaching up to 133 mD (Table 4) [9,98,99].

3.2.2. Naturally Fractured Reservoirs

Tectonic compression and inversion during Late Paleozoic and Mesozoic stages induced the fracturing of rigid carbonate units and basement highs, generating fracture porosity that later served as migration pathways and secondary reservoir systems. These tectonic events strongly controlled the spatial distribution and reservoir quality of fractured intervals. Naturally fractured reservoirs are predominantly found in Early Carboniferous crystalline limestones and sandy-argillaceous formations, which generally exhibit low to moderate reservoir quality (Table 4). Limestones are affected by both primary (tectonic) and secondary (fracture-related) porosity systems. Primary fracturing has been identified in lower Serpukhovian strata at the Ucharal structure, where thin (<5 m) limestone interbeds host minor gas accumulations. These intervals contain meandering fractures partially filled with detrital material. Porosity reaches up to 7%, and permeability is typically below 0.5 mD. Secondary fracturing has been observed across various Early Carboniferous units, with substantial heterogeneity in reservoir quality even within individual structures. Porosity ranges from 3% to 21.6%, while permeability can reach up to 190 mD. Along basin flanks, post-depositional cementation has transformed fractured intervals into low-porosity, impermeable units. Additionally, fractured Proterozoic basement rocks exposed beneath Famennian evaporites at Ortalyk structure in the Kokpansor Trough are of particular interest due to a discovered gas occurrence. This accumulation likely reflects secondary lateral migration from Devonian to Early Carboniferous source intervals rather

than an independent petroleum system, emphasizing the potential of pre-Devonian units as unconventional reservoirs in structurally favorable settings [9,38,56,95,99].

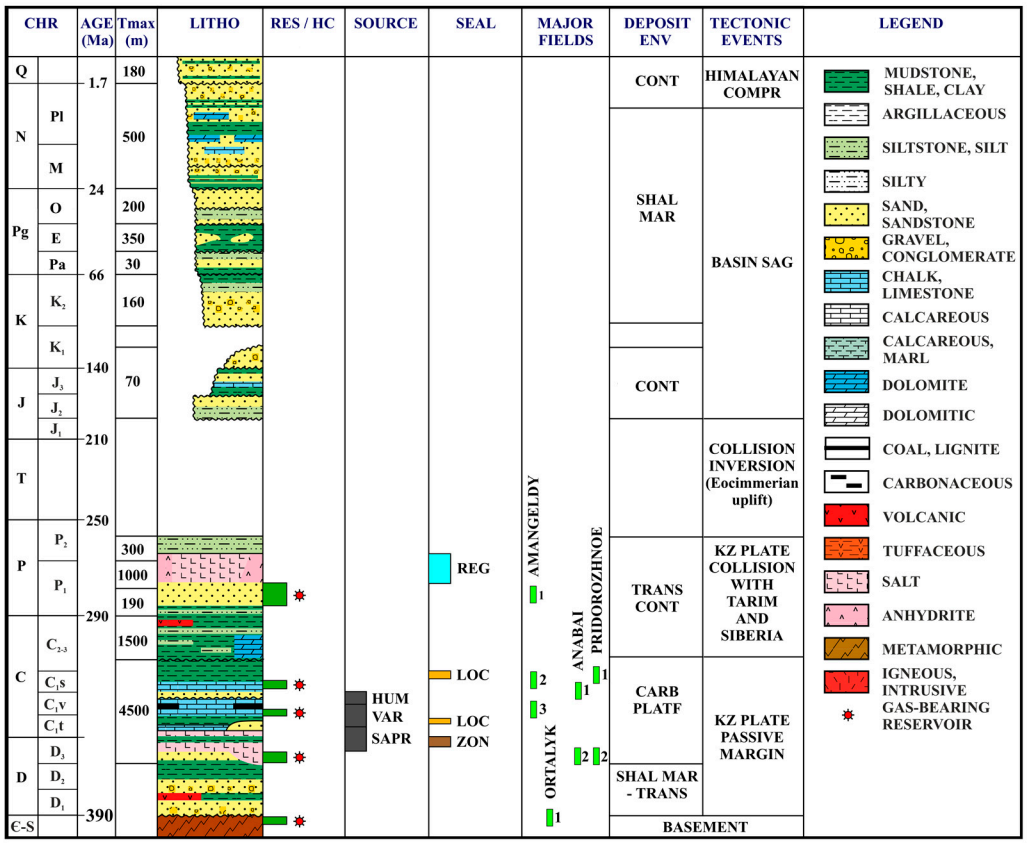


Figure 7. Chrono- and lithostratigraphic chart illustrating tectonic–depositional evolution and petroleum system elements in the Shu-Sarysu Basin (modified after [28,29]). Chrono—chronostratigraphy; T—thickness; HC—hydrocarbons; Q—Quaternary; **N—Neogene:** Pl—Pliocene; M—Miocene; **Pg—Paleogene:** O—Oligocene; E—Eocene; Pa—Paleocene; **K—Cretaceous:** K_1—Early Cretaceous; K_2—Late Cretaceous; **J—Jurassic:** J_1—Early Jurassic; J_2—Middle Jurassic; J_3—Late Jurassic; **T—Triassic:** T_1—Early Triassic; T_2—Middle Triassic; T_3—Late Triassic; **P—Permian:** P_1—Early Permian; P_2—Late Permian; **C—Carboniferous:** C_1—Early Carboniferous: C_1t—Tournaisian; C_1v—Visean; C_1s—Serpukhovian; $C_{2\text{-}3}$—Middle–Late Carboniferous; **D—Devonian:** D_1—Early Devonian; D_2—Middle Devonian; D_3—Late Devonian; **Є-S—Cambrian–Silurian**; Sun symbol—gas-bearing reservoir; lithological symbols are shown in the legend at right; **DEPOSIT ENV—Depositional environments:** CONT—continental; SHAL MAR—shallow marine; TRANS CONT—transitional to continental; CARB PLATF—carbonate platform; SHAL MAR—TRANS—shallow marine to transitional; **Tectonic events:** HIMALAYAN COMPR—Himalayan compression; BASIN SAG—Sag phase; COLLISION INVERSION—tectonic inversion; KZ PLATE COLLISION WITH TARIM AND SIBERIA—Kazakhstan Plate collides with Tarim and converges with Siberia plates; KZ PLATE PASSIVE MARGIN—passive margin of Kazakhstan Plate; blank fields—stratigraphic hiatus due to uplift, erosion, or absence of preserved deposits: Triassic–Early Jurassic reflects regional uplift during Eocimmerian tectonics; middle Cretaceous indicates localized erosion.

3.2.3. Hybrid Porous-Fractured Reservoirs

Hybrid reservoirs developed in structurally complex zones where tectonic uplift and compaction enhanced microfracturing in otherwise low-porosity formations. Interaction between tectonic fracturing and sedimentary facies led to heterogeneous porosity–permeability systems with commercial gas potential. A transitional class of reservoirs of Tournaisian to Permian age is recognized within the DPS, characterized by moderate porosity, microfracturing, and variable permeability. These hybrid porous-fractured sys-

tems differ from both conventional and fracture-dominated reservoirs and are associated with industrial gas inflows. Representative examples include the Ortalyk field (Permian, Kokpansor Trough), Amangeldy and North Ucharal (Permian), and Airakty and Maldybai (Tournaisian-early Visean) in the Moiynkum Trough (Figure 1). These reservoirs typically consist of sandy siltstones and, to a lesser extent, carbonate rocks. Porosity ranges from 6% to 12%, and permeability reaches up to 1.0 mD [9,99,100].

Table 4. Stratigraphic distribution and properties of reservoir types in the Shu-Sarysu Basin. P_1—Early Permian; C_{2-3}—Middle–Late Carboniferous; C_1v_2-s—Late Visean–Serpukhovian (Early Carboniferous); C_1t-v_1—Tournaisian–Early Visean (early Carboniferous); D_3fm—Famennian (Late Devonian).

Age	Extent	Lithology	Thickness (m)	Type	Porosity (%)	Permeability (mD)
P_1	Regional	Sandstone	15–50	Non-fractured	19–22	133
P_1	Local	Sandstone, siltstone	≤45	Mixed	6–12	≤1
C_{2-3}	Regional	Sandstone	≤50	Non-fractured	3–10	up to 1
C_1v_2-s	Local	Limestone, sandstone	≤26	Mixed	10–14	146
C_1v_2-s	Local	Sandstone, siltstone	≤5	Fractured	≤7	≤several dozens
C_1v_2-s	Local	Limestone	≤100	Fractured	≤3	≤several dozens
C_1t_1-v_1	Local	Carbonates, sandstone, siltstone	20–50	Mixed	6–13.6	≤2
C_1t_1-v_1	Zonal	Sandstone	20–50	Non-fractured	3–21.6	≤190
D_3fm	Zonal	Sandstone	40–100	Non-fractured	7–26.9	≤12

3.2.4. Diagenetic Alteration and Its Control on Reservoir Quality

The evolution of reservoir properties in the Shu-Sarysu Basin (SSB) was significantly influenced by diagenetic processes, which operated throughout the Devonian–Permian stratigraphic intervals. While structural and depositional controls have been emphasized in previous sections, diagenetic alterations such as cementation, dissolution, compaction, and recrystallization played a crucial role in modifying primary porosity and permeability, particularly in sandstones and carbonates [101].

Thermal and X-ray diffraction analyses of Carboniferous–Permian rocks in the southwestern SSB revealed widespread occurrences of quartz, feldspar, phyllosilicates (including hydromica and chlorite), and carbonates, minerals that actively participate in diagenetic transformations [97]. Organic matter localization within clay mineral structures (e.g., montmorillonites) and microcrystalline calcite was identified as a key factor affecting both reservoir quality and hydrocarbon generation. Dispersed organic matter concentrations reached up to 2% in feldspar-rich terrigenous rocks, indicating potential for enhanced thermal cracking under catagenetic conditions.

The occurrence of authigenic smectite, palygorskite, and illite suggests volcanogenic and hydromorphic diagenesis, linked to meteoric and alkaline fluid interactions in semi-arid episodes [102]. Furthermore, microfacies analysis indicates spatial variability in cementation across lagoonal and shoal environments, which influenced porosity retention and secondary porosity zones [39].

In carbonate units, diagenetic features such as microfracturing, stylolite formation, and secondary porosity due to calcite dissolution have been observed. These processes locally improved reservoir quality, especially in early Visean limestones of the Moiynkum and Tasbulak troughs. However, pervasive calcite and silica cementation often occluded pore spaces in marginal facies, reducing effective porosity to <5% [97].

The presence of mixed-layer clays and thermal inert minerals (e.g., thermally amorphous quartz) also influenced diagenetic paths. The detection of mixed-layer minerals and secondary chlorite indicates late-stage diagenetic recrystallization, which is typically associated with burial depths >3.5 km and elevated paleo-geothermal gradients [97].

In summary, diagenesis exerted both constructive and destructive controls on reservoir development in the SSB. Zones of enhanced secondary porosity, particularly in the Visean and Famennian intervals, are critical targets for exploration. Conversely, areas with extensive diagenetic cementation should be treated with caution due to poor reservoir performance.

3.3. Seals

HC entrapment and preservation within the SSB were predominantly governed by the distribution and effectiveness of regional, zonal, and local seals, primarily composed of evaporitic deposits (Table 5). In stratigraphic intervals lacking these sealing facies, primary accumulations were likely breached, resulting in vertical migration of gas. Conversely, where competent seal formations are present in the upper stratigraphic section (Visean–Permian; see Table 5 and Figure 8), this process enabled the formation and preservation of secondary accumulations, as exemplified by the Amangeldy and Airakty gas fields. The spatial distribution, continuity, and lithological composition of sealing formations were largely shaped by tectono–sedimentary dynamics throughout the Devonian–Permian evolution. Tectonic subsidence and isolation of restricted lagoons during the Famennian and Early Permian created favorable conditions for evaporite precipitation in structural lows, resulting in thick halite-bearing regional and zonal seals. Conversely, uplifted blocks and syntectonic erosion limited seal development in marginal zones, leading to a potential seal breach or vertical leakage. Differential subsidence and sediment infill during Visean–Serpukhovian transgressive–regressive cycles controlled the deposition of local clay–sulfate seals, especially in structurally segmented areas such as the Lower Shu Uplift and Moiynkum Trough.

Table 5. Distribution of sealing units in the Devonian–Permian succession of the Shu-Sarysu Basin. P_1—Early Permian; C_1v-s—Visean–Serpukhovian (Early Carboniferous); D_1fm—Famennian (Late Devonian).

Stratigraphic Interval	Type and Composition	Average Thickness (m)
P_1	Regional seal (continental evaporitic/halite-bearing)	~1000
C_1v_1-s_2	Local seals (sulfate–argillaceous)	~300
D_1fm	Zonal seal (lagoonal evaporitic/halite-bearing)	~500

The Early Permian evaporitic formations are regionally distributed across the SSB, with the exception of uplifted zones such as the Tasty and Bugudzhil uplifts, where evaporite sequences locally reach the surface. In contrast, lagoonal zonal evaporites of Famennian to early Tournaisian age are predominantly developed within the Lower Shu Uplift and the southern sectors of the Kokpansor and Tasbulak troughs (Figure 8). Shales and evaporites of Early Carboniferous age, occurring between Famennian zonal and Early Permian regional seals, constitute local sealing units. These intervals are primarily developed within Serpukhovian and Visean sediments of Lower Shu Uplift, the northwestern part of Moiynkum Trough (Amangeldy and Airakty fields), and the southern sector of Tasbulak Trough (Figure 9) [101–105].

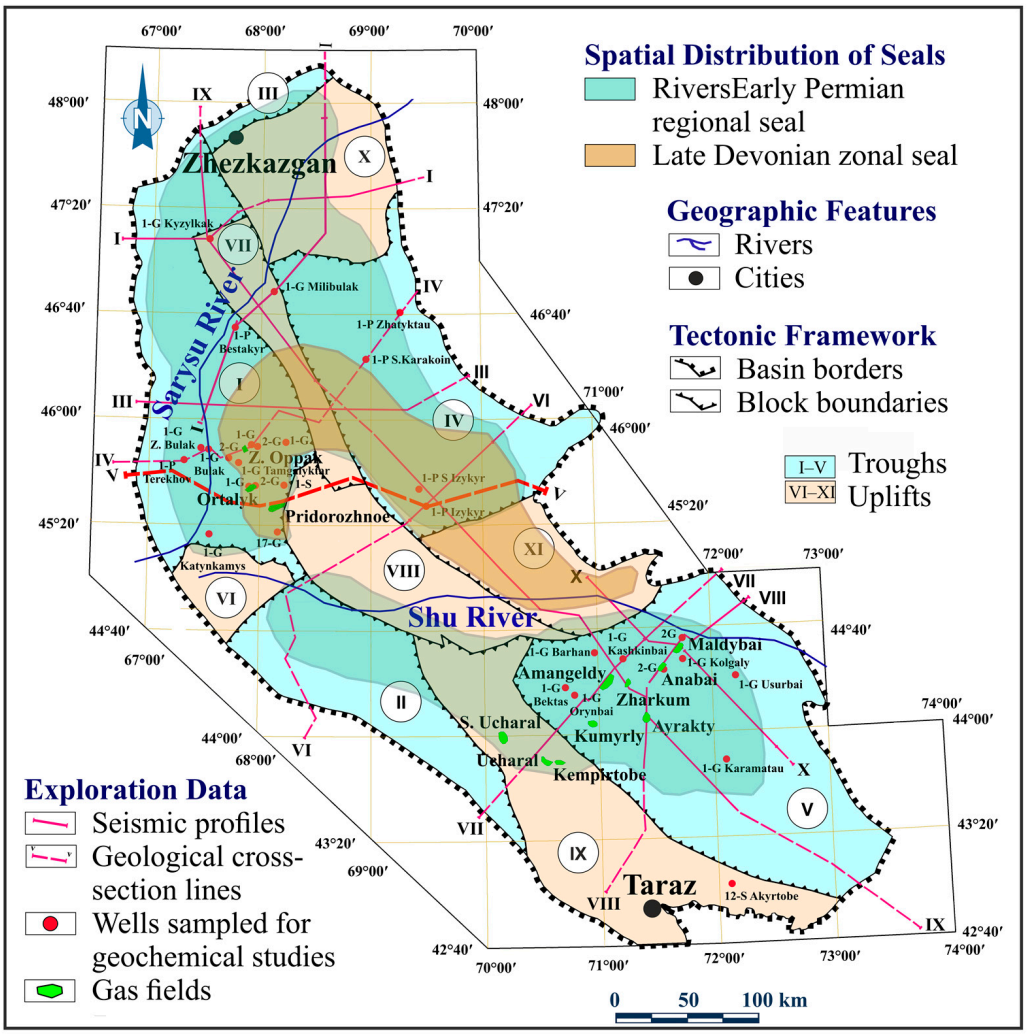


Figure 8. Map showing regional and zonal seal distribution in Shu-Sarysu Basin (modified after [1,14,45]). **Spatial distribution of seals:** blue transparent fill—Early Permian regional seal; brown transparent fill—Late Devonian zonal seal; other abbreviations are as in Figure 1.

3.4. Structural Features and Traps

3.4.1. Structural Configuration of the Basement

Basement of the SSB is intensely faulted and segmented into a mosaic of uplifted and downthrown blocks shaped by successive tectonic episodes during the Paleozoic and Mesozoic, including Hercynian and post-orogenic reactivation phases. Prominent structural highs are exposed in bordering ranges (Ulytau, Karatau, Kyrgyz Alatau), as well as in intrabasinal features such as Kendyktas, Shu block, and anticlinoria including Ergenekty–Zhuantobe. Deep wells have also penetrated basement complexes in several internal troughs (Figure 4). Based on geophysical and drilling data, the basement is subdivided into major structural blocks with contrasting vertical displacements (Figure 1; Table 6). These structural foundations exert primary control on overlying sedimentary architecture and determine spatial distribution and style of structural traps, as well as influence lateral migration pathways of fluids and gases [106–108].

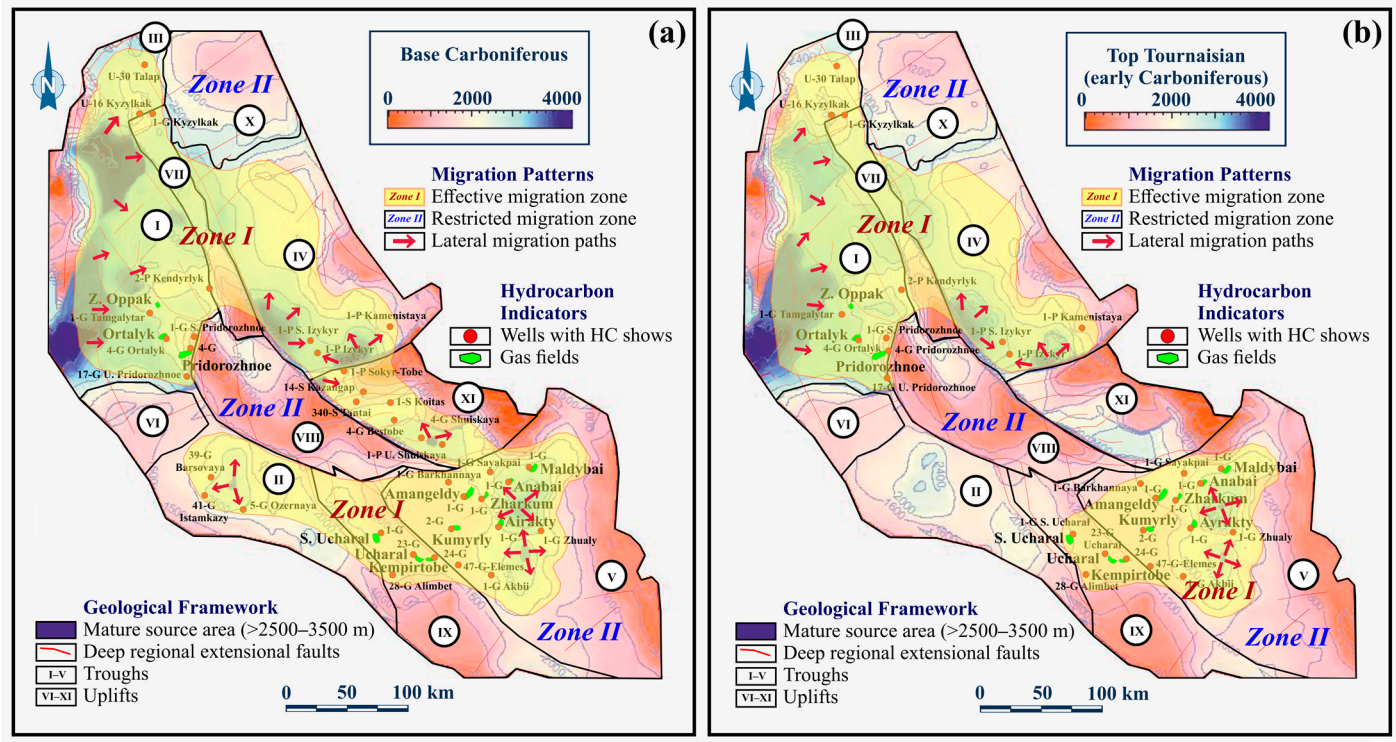


Figure 9. Spatial patterns of source rock maturity, inferred migration pathways, and geological success probability zones within (**a**) Late Devonian and (**b**) Early Carboniferous intervals of the Shu-Sarysu Basin (modified after [14,28,45,97–109]). **Migration patterns:** Zone I (yellow transparent fill)—effective migration and accumulation; Zone II—restricted migration; yellow arrows—lateral migration paths; **hydrocarbon indicators:** red circles—wells with hydrocarbons (HC) shows; green polygons—gas fields; **geological framework:** blue fill—potentially mature source area (>2500–3500 m); solid red lines—deep regional extensional faults; I–XI—troughs and uplifts as in Figure 1. **Interpretive note:** Zones I and II correspond to areas of relatively high and reduced geological success probability, respectively, based on petroleum system element functionality and structural configuration.

Table 6. Depth ranges of major basement blocks in the Shu-Sarysu Basin.

Block Name	Type	Absolute Depth Range (m)
Kokpansor Block	Through	−2500 to −4500
Sozak-Baikadam Block	Through	−2500 to −3500
Zhezkazgan Block	Through	−1200 to −2500
Tasbulak Block	Through	−2000 to −5500
Moiynkum Block	Through	−1500 to −4000
Bugudzhil Block	Uplift	−1500 to −2500
Betpakdala Block	Uplift	−1500 to −3500
Tasty Block	Uplift	0 to −1500
Talas Block	Uplift	−1500 to −3000
Sarysu Block	Uplift	−500 to −2500
Lower-Shu Block	Uplift	−1500 to −4000

Tectonic segmentation of the basement established the primary structural template that guided syn-depositional accommodation space and influenced facies distribution across the overlying DPS. Long-lived structural highs promoted erosion or reduced sedimentation, whereas subsiding blocks accumulated thick successions conducive to the development of source rocks, reservoirs, and seals in a stacked configuration.

3.4.2. Tectonic Zonation and Structural Elements

The central part of the SSB is controlled by a regional NW-SE trending uplift system comprising Betpakdala, Tasty, and Talas uplifts, which separate Kokpansor and Sozak-Baikadam troughs in the southwest from Zhezkazgan, Tasbulak, and Moiynkum troughs in the northeast (Figure 1). Hereinafter, the term "trough" refers to intracontinental structural depressions developed within the sedimentary cover of the SSB, and is not used in the context of oceanic subduction-related troughs. Each structural unit displays distinct morphostructural styles and degrees of fault segmentation [1,28,45,49,80,109–111]:

- The Kokpansor Trough is defined by intense block faulting and includes features such as the Oppak Uplift and Zhapraktinskaya syncline, representing a highly prospective domain for structural traps associated with rotated fault blocks and local folding (Figure 1);
- The Sozak-Baikadam Trough exhibits relatively simple geometry and moderate faulting. Broad synclinal structures such as Sozak and Baikadam depressions dominate, with potential anticlinal and fault-related traps along block boundaries (Figure 1);
- The Moiynkum Trough is a wide, segmented block with contrasting southwestern (gently folded) and northeastern (faulted) zones, which hosts fault-bound swells and synclines including Airakty and Maldybai structures, associated with known gas accumulations (Figure 1);
- The Tasbulak Trough is structurally less deformed and contains limited anticlinal features with main structures concentrated along the northeastern margin, where high-amplitude anticlines are linked to compressional faulting (Figure 1);
- The Zhezkazgan Trough is a narrow, fault-bounded monocline with minimal internal deformation and exploration potential related to proximity to mature source rocks and carrier systems (Figure 1);
- The Bugudzhil Uplift is a structurally elevated block between Kokpansor and Sozak-Baikadam troughs that, although poorly studied, may play a key role in regional fluid migration pathways (Figure 1);
- The Betpakdala Uplift extends northeast from the Tasty Uplift and comprises faulted swells and steps (Ortasynyrly, Milibulak), functioning as a boundary zone that contributes to trap closure (Figure 1);
- The Tasty Uplift is a NW-trending ridge segmented by strike-slip and transverse faults that exerts major structural control on basin configuration and delineates petroleum system domains (Figure 1);
- The Talas Uplift forms the western margin of the Moiynkum Trough and is composed of faulted anticlines and ridges (eKoskuduk-Norbay), serving as a localized trap zone influenced by shear faulting (Figure 1);
- The Sarysu Uplift is a dome-shaped structural high north of the Tasbulak Trough centered on the Central Sarysu Arch (up to 300 m), where fault segmentation and associated brachyanticlines govern local migration and trap development (Figure 1);
- Lower Shu Uplift is a transitional zone between Moiynkum and Tasbulak troughs characterized by subdued topography and cross-cutting high-amplitude faults potentially facilitating lateral HC migration (Figure 1).

The outlined structural zonation reflects a compound history of extension, compression, and inversion, which collectively shaped the basin's petroleum systems. These tectonic regimes controlled syn-sedimentary thickness variations and depositional facies patterns, ultimately governing the location, style, and preservation potential of structural traps.

3.4.3. Post-Paleozoic Structural Modifications

Mesozoic and Cenozoic tectonic overprints modified surface morphology but exerted limited control on integrity of Paleozoic traps. The only significant post-Paleozoic structure is the Sozak Trough, infilled with Cenozoic sediments and bounded by Karatau Fault. Although this feature does not directly affect Devonian–Permian traps, it locally affects overburden thickness and geothermal gradients [21,78].

3.4.4. Trap Types

The origin and spatial configuration of traps in the SSB are inherently tied to tectono–sedimentary interactions during basin formation. Episodes of subsidence enabled accommodation for reservoir and seal deposition, while compressional and transtensional regimes defined trap geometries and their structural integrity. The structural framework of the SSB defines a range of trap types, including faulted anticlines, tilted fault blocks, compressional folds, and flexural structures (Table 7). These traps predominantly formed along marginal zones of basin troughs, where subsided structural elements were later reactivated through fault segmentation and inversion processes. However, internally developed traps also originated within deeper central parts during Early Paleozoic compressional phases, primarily as low-amplitude anticlines and flexural features associated with differential subsidence and inherited basement morphology. While marginal structures are more numerous, they often experienced partial disruption due to Mesozoic–Cenozoic tectonic reactivation. In contrast, most closures within deeper central parts of the troughs remain preserved due to greater burial depth, thicker evaporite seals, and reduced post-Paleozoic disturbance [1,9,28,112]. Trap effectiveness across the basin varies with burial depth, fault architecture, and seal continuity.

Table 7. Summary of structural trap types and their occurrence in the Shu-Sarysu Basin.

Trap Type	Structural Setting	Typical Location	Notes
Anticlines (Late Paleozoic)	Compression	Flanks of major troughs	Low- to moderate-amplitude folds often aligned with inherited basement highs; typically flexural in style
Brachyanticlinal folds (Paleozoic–Mesozoic)	Mild compression	Central and marginal uplift zones	Typically low-relief, with moderate closure
Fault-related folds (Permian–Triassic)	Associated with reverse or strike-slip faults	Faulted margins of blocks	Often show flexural style, enhanced by fault drag
Tilted fault blocks (Mesozoic)	Normal faulting with block rotation	Trough margins	Common in Kokpansor and Moiynkum troughs
Flexural synclines (Late Paleozoic–Mesozoic)	Compression-induced flexure	Between uplift and trough transitions	May act as stratigraphic or combination traps depending on sealing
Compressional anticlines (Late Paleozoic)	High-amplitude folding due to collision	Tasbulak, Talas, Tasty uplifts	High-amplitude folds formed by crustal shortening, distinct from flexural anticlines; characterized by multiple closures; poorly imaged by shallow seismic

3.5. Hydrocarbon Migration and Geological Success Zones

The SSB exhibits a segmented hydrodynamic architecture, a system of isolated troughs characterized by predominantly stagnant (elision-type) fluid regimes which hinder lateral flow and promote localized vertical migration of fluids [46,113,114]. This compartmentalization is evidenced by substantial variations in formation pressures up to 40%, recorded within the same stratigraphic intervals across different fields. Migration pathways evolved

under the influence of multiphase tectonic activity and restricted fluid flow within Famennian, Tournaisian, and Visean strata, followed by vertical migration through fault systems into Lower Permian reservoirs interpreted as structurally reactivated faults that acted as vertical conduits following initial compressional deformation [14]. HC generation centers developed within deeply buried thermally mature marine and coal-bearing successions in the troughs of SSB. These troughs functioned as independent HC kitchens during Late Devonian and Early Carboniferous time, with generation proceeding under limited hydrodynamic connectivity and high sealing efficiency [109]. Vertical migration into overlying Permian strata was constrained by laterally extensive evaporitic seals, effectively preserving HC within pre-Permian carrier and reservoir systems (Figure 9). Diagenetic modifications, especially pervasive cementation and compaction in marginal facies, may have created migration barriers or diverted flow paths. Conversely, zones of dissolution and microfracturing provided high-permeability channels facilitating upward and lateral migration.

Two principal gas-bearing intervals are recognized in the SSB [14,28,97]:

- The lower interval is associated with organic-rich Famennian and Early Carboniferous successions, where effective generation occurred within the axial zones of troughs, followed by lateral updip migration toward flanking structural traps. Migration is assumed to proceed predominantly updip along stratigraphic surfaces toward structural highs, given the limited structural control observed in available fault data.
- The upper interval corresponds to Lower Permian red-colored deposits that lack mature source rocks and were primarily charged through secondary vertical migration. This process was likely triggered by tectonic reactivation and increased geothermal gradients during the Permian, occasionally accompanied by partial seal breach.

Direct evidence of HC migration and accumulation includes gas-bearing intervals encountered in wells, geochemical indicators, and gas shows in fractured limestones [9,109]. Particularly notable is the semicircular distribution of accumulations along the flanks of the Moiynkum and Trough, indicating updip migration from deepend generation centers into stratigraphic or combination traps formed along reservoir pinch-outs and facies transitions.

Drilling data confirm the presence of gas shows in several underexplored structures. In the Tasbulak Trough, these are concentrated in the southwestern and central segments. In the southeastern Moiynkum area, gas manifestations occur outside active exploration zones. In the Zhezkazgan and Sozak-Baikadam areas, elevated structural blocks with gas shows are observed within Lower Permian, Serpukhovian-Visean, and Lower to Middle Carboniferous successions [9]. These findings support the presence of active source centers and functioning migration pathways despite limited exploration coverage.

Based on geological and hydrodynamic analysis, two principal migration–accumulation zones were delineated for each stratigraphic interval (Figure 10) [14,28,97].

Zone I includes areas with burial depths of 2500–3500 m, thermally mature source rocks, and laterally connected pathways toward structural traps. It hosts proven gas accumulations such as the Amangeldy, Airakty, Zharkum, and Maldybai fields, as well as shallow gas shows in fractured limestones:

- In the Late Devonian interval (Figure 9a), Zone I comprises the Kokpansor Trough, southern and western Tasbulak Trough, northern and western Moiynkum Trough, northern Sozak–Baikadam Trough, Betpakdala Uplift, northern Talas Uplift, and Lower Shu Uplift.
- In the Early Carboniferous interval (Figure 9b), it includes the Kokpansor, Tasbulak (south and west), and Moiynkum (north and west) troughs, Betpakdala Uplift, and northern Talas Uplift.

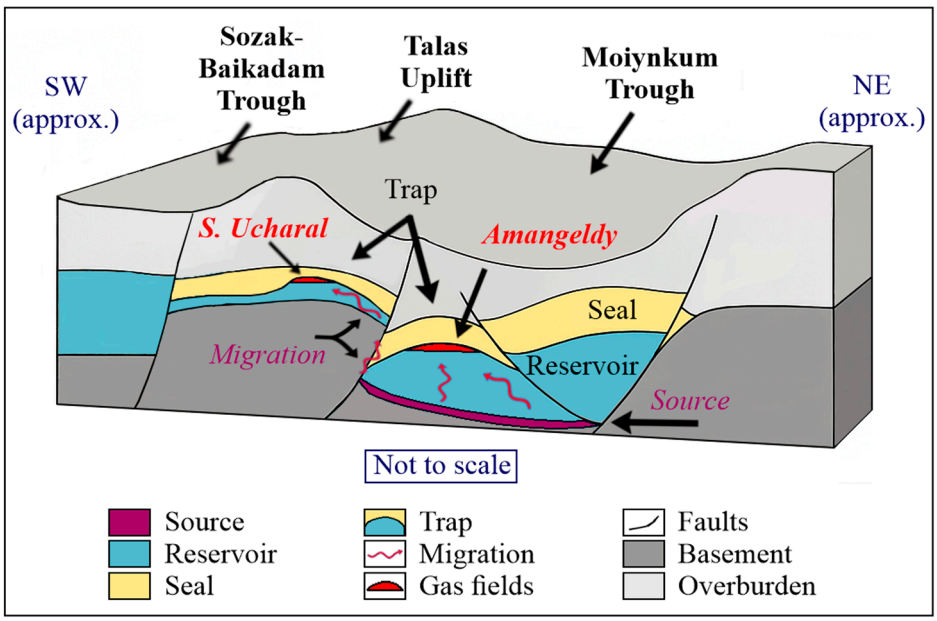


Figure 10. Conceptual 3D schematic of petroleum system architecture across the Sozak-Baikadam Trough, Talas Uplift, and Moiynkum Trough. **Petroleum system elements:** purple fill—source rocks; blue fill—reservoir rocks; yellow fill—seals; light ochre lens—traps; wavy purple arrows—hydrocarbon migration paths; red caps—confirmed gas fields (e.g., Amangeldy, S. Ucharal); **structural and geological features:** black lines—faults; dark grey fill—basement; light grey fill—overburden.

Zone II, comprising the rest of the basin in each interval, is characterized by lower seal quality, discontinuous aquifers, and poor lateral connectivity. These conditions limited hydrocarbon migration and trapping, often resulting in dispersed or thermally degraded accumulations. Notably, the Sozak-Baikadam Trough and Lower Shu Uplift, part of Zone I in the Devonian, fall into Zone II in the Carboniferous due to reduced sealing integrity and increased compartmentalization.

Based on the integration of petroleum system elements, such as source rock maturity, migration efficiency, trap configuration, and seal continuity, the delineated Zones I and II represent areas of relatively high and reduced geological success probability, respectively. This interpretation follows frameworks applied in previous basin-scale assessments [115–122], where system functionality guides spatial classification of exploration risk.

Although the analysis delineates migration–accumulation zones across major stratigraphic intervals, it should be noted that migration pathways and trap integrity in several underexplored zones remain hypothetical due to incomplete structural imaging and sparse well intersections. Interpretations for such areas should be regarded as preliminary. These observations highlight pronounced spatial heterogeneity in source maturity, migration efficiency, and trap preservation across the basin, governed by stratigraphic discontinuities, structural segmentation, and contrasting hydrogeological regimes.

4. Discussion

This section presents interpretations of the results of two main tasks, considered in the context of underexplored regions and limited exploration maturity. This study integrates Soviet-era and recent data into a unified synthesis, re-evaluated through modern petroleum systems analysis.

4.1. Exploration Maturity

As shown in previous sections, geological exploration across the SSB remains spatially uneven. Drilling and seismic surveys have been concentrated in a few structurally favorable zones, while large areas remain poorly investigated. The interpretation of petroleum system elements in these regions is complicated by the predominance of analog-format seismic and well logging data, which limits their applicability in modern workflows. Geochemical datasets are also spatially fragmented and often rely on outdated or low-resolution methods, with only a few zones benefiting from modern core-based analysis. This fragmented and inconsistent dataset presents significant challenges for reconstructing continuous migration pathways, evaluating trap integrity, and assessing generative maturity—especially in structurally isolated or data-poor segments of the basin.

Despite these constraints, the integrative approach applied in this study—combining basin evolution with petroleum system analysis—proved effective for synthesizing heterogeneous data and identifying structurally and thermally favorable zones. It enabled the delineation of prospective areas even under limited data conditions by leveraging analogs and regional geological patterns. However, the approach is not without limitations. In areas lacking seismic imaging or reliable well control, conclusions remain tentative and biased toward better-studied regions.

Several interpretations, such as delineation of petroleum system functionality at the basin scale, are partially based on extrapolation from better-studied zones. Therefore, areas with limited control should be treated as provisional until additional data become available. Explicit differentiation between data-supported findings and hypothesis-driven extensions has been introduced in relevant sections. The persistent uncertainty in data-scarce sectors underscores the need for systematic digitization of legacy records and the application of advanced computational modeling to enable more robust, basin-wide interpretations.

4.2. Spatiotemporal Evolution of Devonian–Permian Petroleum Systems in the Geological Context

The basin's petroleum systems evolved under the direct control of tectonic subsidence phases and associated sedimentary environments. The timing, intensity, and spatial configuration of tectonic events strongly influenced the distribution and characteristics of source rocks, reservoirs, and seals. The tectono-stratigraphic evolution of the SSB reveals distinct spatial controls on petroleum system elements. Alternating phases of transgression, regression, tectonic uplift, and sagging gave rise to variable depositional environments that shaped source rocks, reservoirs, and seals. Devonian evaporitic settings formed under local arid climate and tectonic quiescence, producing halite-bearing sequences with zonal distribution and limited vertical continuity. In contrast, regionally extensive top-seal units are associated with Lower Permian evaporites, whereas localized low-efficiency sulfate seals also formed within Lower Carboniferous settings. Tournaisian-Visean transgression enabled widespread deposition of organic-rich marine facies and carbonates, analogous to settings in the Turgay and Syr-Darya basins, which are considered potential source rocks based on regional analogs and preserved TOC trends.

Subsequent regression during the Serpukhovian led to increased clastic input, compartmentalizing earlier marine sequences. This marked a transition from widespread marine settings to more compartmentalized depositional environments. For Permian structural segmentation-controlled facies belts, troughs accumulated saline lacustrine deposits with efficient seals, while marginal zones showed thinning and lithological variability. This contrast is greater than in neighboring basins with more stable subsidence histories. Although post-Paleozoic tectonics modified surface structures, key Devonian–Permian petroleum system elements, and thus the hydrocarbon potential, remain largely preserved.

Collectively, the internal heterogeneity and structural inheritance of the SSB, distinguish it from simpler platform-type systems and enhance its exploration significance.

4.3. Source Rocks and Thermal Maturity

The study of source rock evolution in the SSB, particularly within Devonian–Early Carboniferous successions, suggests the realization of effective gas-prone petroleum systems. The transition from early qualitative methods (bitumen analysis, gasometry) to quantitative approaches (Rock-Eval pyrolysis, Ro, and PI) enabled more accurate assessment of organic matter characteristics and maturity levels. Whereas earlier studies merely indicated the presence of bitumen, recent data suggest that Late Meso to Apocatagenesis stages were reached, corresponding to advanced phases of gas generation [14].

Maturity indicators in the Moiynkum Trough (Tmax up to 579 °C, Ro up to 3.3%) are consistent with results reported by Seithaziyev (2023) for Amangeldy and Airakty fields, where gas maturity exceeds that of associated condensates. Isolated samples exhibit TOC values reaching up to 23%, supporting interpretation of originally high generative potential prior to thermal overmaturation. These data confirm late gas migration and full realization of source rock potential.

Analysis of maturity and residual organic content across troughs (Table 2) suggests that gas generation was most prominent in the Moiynkum Trough. In the Tasbulak Trough, organic matter depletion is observed under high maturity conditions, whereas in the Kokpansor Trough, isolated generative zones persist under moderate maturity (Table 2). Comparisons with calculations following [42] indicate that without correction of TOC values, mature intervals would be erroneously classified as low potential. Application of lithology-based correction factors (1.6–2.0) allows more accurate scaling of generative capacity, particularly in deeper parts of southern troughs (at depths exceeding 3000–3500 m), where Rock-Eval results show depleted kerogen but residual gas potential remains.

Thermal maturity varies laterally across the basin, with measured vitrinite reflectance values ranging from 1.39% to 3.3% and Tmax between 300 and 579 °C, indicating stages from Late Mesocatagenesis to Apocatagenesis (Table 2). According to generalizations, southern segments of basin reached Apocatagenesis stages (up to coalification levels), while northern areas remained within Late Mesocatagenesis. This pattern suggests a tendency toward phase differentiation, where gas-dominated systems prevail in the south, while northern regions may retain conditions more favorable for liquid HC generation. Helium contents of up to 0.83% recorded in Moiynkum gases support interpretations of deep fluid origins and high source maturity, serving as additional evidence of a late gas system. Overall, the gas-prone character of the SSB is reinforced by exploration drilling results and laboratory analyses of reservoir fluids.

Data from Tables 2 and 3 and graphical plots (Figures 6 and 7) collectively suggest that petroleum systems within SSB troughs were likely fully developed. Indicators of advanced maturity and residual generative potential are observed. DPS likely evolved under unified thermal impulse, with principal gas generation linked to Visean coal-bearing sequences, while Devonian and Permian deposits provided secondary generative and sealing functions. Their stratigraphic coupling and fluid manifestations suggest that a late gas-dominated petroleum system was active across much of basin.

Statistical TOC parameters reveal significant heterogeneity in organic matter distribution across the basin. TOCmean values exceeding 1.5% in Visean coal-bearing intervals of the NE Moiynkum Trough and Lower Shu Uplift support fair to good gas-source potential under mature conditions. TOCmax values above 4%, and locally reaching up to 22.97%, indicate the presence of isolated high-quality source intervals with originally elevated generative capacity. In contrast, TOCmin values below 0.3% in Early Permian

marls reflect low organic richness and likely sealing or non-generative functions. This spatial variation correlates with tectonic segmentation, subsidence patterns, and paleogeographic controls—supporting the interpretation of compartmentalized but fully developed gas-prone petroleum systems throughout the basin. At the same time, in areas where direct Rock-Eval or Ro data are unavailable, maturity levels and generative potential are inferred from stratigraphic position and regional analogs. This introduces interpretive uncertainty that must be acknowledged when extending findings across structurally complex or underexplored zones.

4.4. Reservoir Rocks and Seals

The distribution of reservoirs and seals within the SSB reflects the combined influence of tectonic segmentation, sedimentary dynamics, and paleogeographic evolution. Transgressive episodes during Famennian-Visean and widespread evaporite deposition in Early Permian played a critical role in establishing conditions favorable for both reservoir development and sealing. HC accumulations are primarily hosted in porous and fractured terrigenous reservoirs, predominantly sandstones and siltstones, within Tournaisian, Visean, and Lower Permian formations, with the best development recorded in Moiynkum and Kokpansor troughs. Fractured and cavernous carbonate reservoirs are mostly confined to upper Visean and Serpukhovian intervals. Although secondary accumulations have been observed within fractured Proterozoic basement overlain by halite (e.g., Ortalyk structure), detailed assessment of this unconventional play falls outside the present study scope. Spatial and stratigraphic analysis of reservoir–seal relationships suggests a zoning pattern across the basin, differentiated by structural setting, reservoir quality, and seal effectiveness, as summarized in Table 8.

Table 8. Exploration zoning based on reservoir–seal distribution and structural setting. C_1-P_1—Early Carboniferous–Early Permian.

Zone Type	Structural Location	Reservoir Characteristics	Seal Type	Prospectivity Level
Most Promising	Inner parts of Kokpansor, Moiynkum, Tasbulak troughs	Multi-level porous and fractured reservoirs (D_3-P_1)	Regional Permian halite, Famennian evaporites	High
Moderately Promising	Slopes of uplifts (Tasty, Talas, Lower-Shu, etc.)	Locally developed Permian and Carboniferous reservoirs	Local and zonal seals	Moderate
Low Prospects	Marginal uplifts, Tasty uplift	Poorly preserved or eroded reservoirs, lack of seals	Absent or ineffective	Low

Most favorable geological conditions are concentrated within deep troughs, where stacked porous reservoirs are overlain by thick Permian halite seals and supplemented by Famennian evaporites and sulfate–clay caps. Fields such as Amangeldy, Airakty, and Pridorozhnoe provide characteristic examples of this favorable configuration. In contrast, uplifted and marginal zones, including the Tasty Uplift and adjacent regions, have been affected by erosion and tectonic inversion, resulting in partial or complete removal of prospective successions and degradation of sealing capacity [70]. Transitional zones, located along flanks of major uplifts and certain sectors of Kokpansor and Tasbulak troughs, preserve partial reservoir–seal pairs but generally lack stratigraphic continuity and reliable sealing integrity (Figure 9). Collectively, these spatial trends highlight the importance of integrating the structural setting, depositional facies, and sealing efficiency in future exploration targeting across the SSB. An integrative understanding of the diagenetic evolution

across the DPS is essential for predicting the heterogeneity of the petroleum system. Cementation, compaction, and dissolution explain the coexistence of productive and tight zones. Mapping diagenetic facies will improve reservoir prediction and migration modeling.

4.5. Structural Features and Traps

The structural framework of the SSB, shaped by multiphase tectonic evolution, including Late Devonian–Carboniferous compression (Hercynian), Permian–Triassic transtensional reorganization, and Mesozoic–Cenozoic extensional faulting, controls the distribution and preservation of HC traps. The basement is segmented into uplifted and downthrown blocks during post-Hercynian transtensional reorganization in the Permian–Triassic, with further modification by Mesozoic extensional faulting, influencing the geometry of overlying DPS. The Kokpansor and Moiynkum troughs exhibit the highest structural complexity, dominated by rotated fault blocks and anticlines, whereas the Tasbulak and Sozak-Baikadam troughs display broader, gentler folding (Figure 9). Uplifts such as Talas and Betpakdala are marked by narrow faulted ridges. While many Paleozoic traps remain intact, uplifted zones show partial erosion. The Sozak Trough, although post-Paleozoic in origin, locally affects overburden thickness and thermal conditions without significantly compromising deeper trap integrity.

Exploration has identified numerous potential structures, but only a few, primarily in the Kokpansor and Moiynkum troughs, are currently drill ready (Figure 9). Structures in Tasbulak, Zhezkazgan, Sozak-Baikadam, and Lower-Shu areas remain under-assessed, with HC indications requiring further evaluation. Trap types, including anticlines, brachyanticlines, fault-related folds, and tilted blocks, are closely linked to inherited tectonic architecture (see Table 7 and Figure 9). Deeper central parts of major basin troughs, where post-Paleozoic disturbance is limited, offer the best preservation conditions. Despite existing structural maps, detailed trap delineation remains limited, particularly in complex and poorly imaged zones. Enhanced seismic interpretation is essential to improve confidence in structural targeting. Thus, the present-day configuration of traps across the SSB is a direct result of inherited structural architecture combined with episodic tectonic reactivation, which also modulated seal effectiveness and trap preservation.

4.6. Hydrocarbon Migration and Geological Success Zones

Petroleum systems of the SSB exhibit significant spatial variability in generative efficiency, migration effectiveness, and preservation potential (Figures 6, 8 and 9). These differences arise from stratigraphic heterogeneity, structural compartmentalization, and contrasting hydrogeological regimes. HC generation was most effective in thermally mature, structurally protected depressions containing marine and coal-bearing source rocks. The Moiynkum, Kokpansor, and Tasbulak troughs demonstrate the clearest alignment between source maturity, lateral migration corridors, and trap integrity, supported by confirmed gas accumulations and preserved system functionality (Table 2).

In contrast, the Sozak-Baikadam and Zhezkazgan troughs show limited evidence of effective charge or retention (Figure 6). Possible explanations include limited exploration coverage and uncertainties related to seal effectiveness, trap closure, or continuity of migration pathways. Given the limited resolution and spatial coverage of mapped fault systems, migration in such areas is assumed to proceed predominantly updip along stratigraphic surfaces toward structural highs. Figure 10 illustrates a conceptual 3D schematic of the petroleum system configuration across representative segments of the basin, emphasizing spatial relationships between mature source rocks, reservoir units, regional seals, and structural traps. The diagram also visualizes inferred hydrocarbon migration pathways and the location of confirmed gas accumulations, such as Amangeldy and S. Ucharal.

A more detailed discussion of migration behavior and petroleum system functionality by structural domain follows below. A shift in migration–accumulation behavior between intervals is also observed in structurally favorable yet stratigraphically variable areas. For instance, while the Sozak–Baikadam Trough and Lower Shu Uplift exhibit characteristics of efficient lateral charge and trap development in the Devonian, their functionality appears diminished in the Carboniferous. This may reflect reduced seal continuity or increased internal compartmentalization, suggesting that even structurally elevated domains can lose system integrity due to subtle changes in stratigraphic architecture or post-depositional overprinting. Tectonic reactivation during the Permian introduced vertical remigration into overlying Permian strata in some areas, suggesting partial seal failure, although preservation remained effective where halogen-bearing seals and low-permeability formations are present.

Overall, the basin contains a spectrum of gas-prone petroleum systems ranging from mature and preserved to partially breached or undercharged. Critical system configuration is interpreted to have been established during the Late Carboniferous to Early Permian, when peak maturation and trap formation overlapped in key structural domains. This supports classification into confirmed systems with demonstrated generative and accumulative integrity (1), prospective zones with favorable geological conditions and indications of gas presence (2), and uncertain domains with unresolved charge and sealing histories (3). These distinctions underscore the need for an integrated structural, geochemical, and hydrodynamic framework to accurately evaluate system effectiveness and guide future exploration within such a compartmentalized basin.

The spatial distinction between Zone I and Zone II, as presented in Figure 9, captures the functional variability of petroleum system elements across the basin. Zone I exhibits a coherent alignment of mature source rocks, effective migration pathways, and confirmed traps, while Zone II is marked by discontinuous flow paths and compromised sealing. This dichotomy reflects differing probabilities of geological success, consistent with established system-based risk zoning approaches.

The interplay of structural segmentation and stratigraphic evolution ultimately shaped the performance and diversity of petroleum systems across the basin.

4.7. Uncertainty and Interpretive Limitations

Petroleum system interpretation across the SSB is critically constrained by uneven subsurface data coverage. Robust assessments are currently limited to a few structurally favorable areas with both seismic and well control, namely, the southeastern Kokpansor Trough, northwestern Moiynkum Trough, central Talas Uplift, and Lower Shu Uplift, where source rock maturity, migration pathways, and trap integrity can be empirically validated.

In contrast, large portions of the basin remain effectively unexplored. The Tasbulak Trough, southern and eastern Moiynkum, northern Kokpansor, Sozak–Baikadam and Zhezkazgan troughs, as well as the Tasty, Sarysu, and Bugudzhil uplifts, lack high-resolution seismic imaging and/or essential well data. Interpretations in these areas are necessarily based on regional extrapolation and analog-derived assumptions, rendering conclusions tentative. Functional attributes such as maturity gradients, migration pathways, and trap configurations are inferred, not observed.

Diagenetic evolution was not explicitly incorporated into the present spatial classification or success probability mapping due to the absence of basin-wide petrographic or mineralogical data. While its significance is recognized, especially in controlling porosity, permeability, and seal integrity, the current resolution of available lithological and geochemical datasets does not support confident delineation of diagenetic facies. As such, the

impact of diagenetic overprint remains a source of interpretive uncertainty in reservoir quality and migration modeling.

In northern and peripheral sectors, thermal regimes remain particularly uncertain due to the complete absence of direct geochemical or temperature measurements. This asymmetry introduces a high risk of interpretive bias toward well-constrained domains, potentially obscuring viable plays or misrepresenting the extent of active petroleum systems. To mitigate this, the study draws a clear distinction between data-supported findings and hypothesis-driven extensions. While regional continuity offers contextual insight, it cannot substitute for empirical evidence when defining generative centers or structural closures.

By pinpointing specific data-deficient zones and qualifying the associated uncertainty, this work establishes a framework for risk-calibrated exploration planning. The proposed three-tier classification reflects not only geological favorability but also data quality and interpretive confidence. Without targeted drilling and modern subsurface imaging, basin-scale conclusions in underexplored areas remain speculative and should be treated accordingly.

5. Conclusions

This review of geological data on the SSB has allowed the systematization of fragmented knowledge accumulated since the 1930s and has provided a coherent understanding of the region's geological evolution. It not only systematizes previously fragmented knowledge but also generates new analytical insights not articulated in the existing literature. Rather than separating data chronologically, the review focuses on integrative reinterpretation of all available information using contemporary geological and petroleum system concepts—this constitutes the core scientific novelty of the work. The following findings reflect the authors' original synthesis based on reinterpretation of published data within a unified analytical framework. They represent results of integrated analysis of legacy and recent data sources reinterpreted in the context of petroleum system analysis, a novel approach not previously applied on a basin-wide scale in the SSB. It formed the basis for reconstructing the spatiotemporal organization and assessing the functional state of petroleum systems within the basin. Synthesizing available information in the context of modern scientific frameworks enabled an objective evaluation of the gas potential of the DPS. The key findings are as follows:

- Despite extensive exploration activities during the Soviet period, the basin remains underexplored. Field operations were concentrated in specific areas, whereas most of the territory exhibits extremely low drilling and seismic survey density. Major data gaps and the lack of modern interpretation approaches continue to limit the assessment of generative potential and trap configuration. Several conclusions, including delineation of mature petroleum systems and trap integrity, are based on analog reasoning and partial data coverage. These interpretations remain provisional in underexplored sectors and are subject to future refinement.
- The geodynamic evolution of the region, involving rift-related, subsidence-driven, and post-orogenic stages, has shaped a stratigraphic framework favorable for the development of petroleum system elements. This interpretation was derived from the comparative spatiotemporal analysis of tectonic phases and facies distribution conducted in the present study. The DPS contains source, reservoir, and sealing facies. Regional seals and favorable facies belts developed under arid climatic conditions and limited marine influence, promoting the preservation of HC accumulations.
- Major fault systems, predominantly extensional and transtensional in nature, have segmented the basin into structural blocks, controlled reservoir architecture, and

locally acted as vertical migration conduits or sealing barriers depending on timing and connectivity.

- Integrated analysis confirms the presence of mature, gas-prone petroleum systems within structurally compartmentalized troughs of the basin. This conclusion is based on maturity data, trap configurations, and seal analyses synthesized from reinterpreted stratigraphic and structural datasets. Spatial alignment between source rocks, reservoirs, and sealing units, along with proven trap integrity, creates favorable conditions for gas accumulation. These results confirm the functionality of mature systems with high generative, migratory, and preservational efficiency. This functional peak is interpreted to have occurred during the Late Carboniferous to Early Permian, when trap formation and hydrocarbon generation were favorably aligned.

Based on source maturity, migration pathways, the presence of effective reservoirs, and the integrity of traps and sealing units within DPS, a classification of exploration areas in the SSB is proposed. These include the following: zones with confirmed functioning systems, such as the Kokpansor and Moiynkum troughs and Talas Uplift (1); geologically favorable areas with documented gas shows, including the Tasbulak, Zhezkazgan, and Sozak-Baikadam troughs, as well as Lower-Shu and Sarysu uplifts (2); and data-deficient domains with unresolved prospectivity, particularly thrust-bound and structurally ambiguous zones (3). Several of these areas, particularly those with documented gas shows, exhibit meaningful potential and should be prioritized in future exploration strategies. At the same time, many local structures remain insufficiently investigated, limiting basin-wide assessments and delaying realization of the full exploration potential. This classification, developed in the present study, constitutes the first basin-wide prospectivity framework based on petroleum system analysis, integrating geological, geochemical, and structural parameters. It offers a practical basis for future exploration prioritization. The delineation of Zones I and II (Figure 9) further supports this classification by representing spatial domains with relatively high and reduced geological success probability, respectively. These zones integrate multiple petroleum system factors, including source maturity, migration efficiency, reservoir presence, and trap integrity, into a spatial framework for exploration risk assessment. This interpretive scheme strengthens basin-wide exploration targeting by linking geological observations to success probability domains. To address this, priority actions include the digitalization of legacy datasets, development of 3D structural models, and refinement of subsurface parameters for key targets, and acquisition of modern geochemical and diagenetic data to better constrain source rock properties, reservoir quality, and migration efficiency.

Author Contributions: Conceptualization, A.Z., A.A., and J.I.; methodology, A.Z. and A.A.; formal analysis, A.Z. and J.I.; investigation, A.Z. and M.T.M.; resources, A.Z. and A.A.; data curation, A.Z.; writing—original draft preparation, A.Z.; writing—review and editing, A.Z., A.A., and J.I.; visualization, A.Z.; supervision, A.A. and M.T.M.; project administration, A.Z.; funding acquisition, A.Z. All authors have read and agreed to the published version of the manuscript.

Funding: This research has been funded by the Science Committee of the Ministry of Science and Higher Education of the Republic of Kazakhstan (Grant No. AP19175313).

Data Availability Statement: No new data were created or analyzed in this study. Data sharing is not applicable to this article.

Conflicts of Interest: The authors declare no conflicts of interest.

Abbreviations

The following abbreviations are used in this manuscript:

DPS	Devonian–Permian Succession
HC	Hydrocarbons
HI	Hydrogen Index
PI	Production Index
Ro	Vitrinite reflectance
SSB	Shu-Sarysu Basin
Tmax	Temperature of maximum hydrocarbon generation
TOC	Total organic carbon

References

1. Zhumagulov, A.S.; Manzari, M.T.; Kezembayeva, G.B.; Nurmakova, S.M.; Mukanov, D.B. Tectonic Evolution and Hydrocarbon Accumulation Controlling Characteristics of the Shu-Sarysu Basin. *News NAS RK Ser. Geol. Technol. Sci.* **2022**, *5*, 289–305. [CrossRef]
2. Dillinger, A.; Chanvry, E.; Bolat, Y.; Fustic, M. Architecture and History of Uranium-Bearing Paleocene–Eocene Strata Deposited on the Eastern Margin of the Peri-Tethys (Chu-Sarysu Basin, South Kazakhstan). *Sediment. Geol.* **2024**, *457*, 106677. [CrossRef]
3. Wu, Y.; Lei, Z.; Li, Q.; Tao, S.; Xiao, Y.; Wang, X.; Zhang, N. Helium Accumulation and Uranium Deposit in the Chu-Sarysu Basin—A Symbiotic Process. In Proceedings of the International Field Exploration and Development Conference 2023, Wuhan, China, 19–21 September 2023; Springer: Singapore, 2024. [CrossRef]
4. Satbayev, K.I. On the Question of Finding Diapir Folds in the Pre-Dzhezkazgan Region. *Sov. Geol.* **1939**, *3*, 75–80.
5. Smirnov, A.V.; Korobkin, V.V. Tectonic Map of Kazakhstan at Scale 1:1,000,000 (Principles, Legend, Geological Structures). *Izv. NAS RK Geol. Ser.* **2003**, *2*, 77–89.
6. Bulekbayev, Z.E.; Vocalevskyi, E.S.; Eskuzhiev, B.A.; Kamalov, S.M.; Korostyshevskyi, M.N.; Kuandykov, B.M.; Kuantaev, N.E.; Marchenko, O.N.; Matloshinsky, N.G.; Nazhmetdinov, A.S.; et al. *Oil & Gas Fields of Kazakhstan. Reference Book*; Information Presentation Center of the Mineral Sector of the Republic of Kazakhstan: Almaty, Kazakhstan, 1996; p. 325.
7. Tleubergenova, A.K.; Umirova, G.K.; Maussymbayeva, A.D.; Portnov, V.S. High-Precision Aeromagnetic Survey along the Geotraverse in the Shu-Sarysu Gas Basin. *Neft i Gaz* **2023**, *3*, 52–67. [CrossRef]
8. Karabalin, U.S. Resource Potential of Kazakhstan's Subsoil: Status, Problems, Innovation Vector of Development and Real Prospects. *Neft i Gaz* **2015**, *3*, 15–24.
9. Zhumagulov, A.S.; Manzari, M.T.; Issayev, S.A. Petroleum Plays and Prospectivity of the Shu-Sarysu Basin. *News NAS RK Ser. Geol. Technol. Sci.* **2022**, *6*, 261–275. [CrossRef]
10. Zhumagulov, A.S.; Ismailova, J.A. Geological and Geophysical Studies and Exploratory Drilling of Paleozoic Sediments in the Tasbulak Graben. *Neft i Gaz* **2023**, *6*, 32–42. [CrossRef]
11. Ageev, B.F. Oil and Gas Prospecting Aimed at the Devonian Subsalt Sediments in the Shu-Sarysu Basin. *OilGasGeo* **1985**, 23–26.
12. Akchulakov, U.A.; Zholtaev, G.Z.; Zhylkaidarov, S.E. *Estimation of Predicted Hydrocarbon Resources of the Republic of Kazakhstan. Oil Gas Condensat*; Nedra: Almaty, Kazakhstan, 2003; p. 212.
13. Tleubergenova, A.; Portnov, V.; Karpenko, O.; Maussymbayeva, A.; Madisheva, R. Prospects for the Detection of Structures with Hydrocarbon Deposits along the Geotraverse in the Shu-Sarysu Sedimentary Basin. *Nauk. Visnyk Natsionalnoho Hirnychoho Universytetu* **2023**, *5*, 27–33. [CrossRef]
14. Zhumagulov, A.S. Geological Structure and Prospects for Oil and Gas Content of the Middle-Upper Paleozoic Deposits of the Tasbulak Trough Based on Geological and Geophysical Data. Ph.D. Thesis, Satbayev University, Almaty, Kazakhstan, 2024.
15. Tleubergenova, A.; Umirova, G.; Karpenko, O. Geoelectrical Model of the Earth's Crust Along the Shu-Sarysu Geotraverse According to Magnetotelluric Soundings. *Nauk. Visn. Nats. Hirn. Univ.* **2023**, *3*, 18–25. [CrossRef]
16. Baibatsha, A.; Vyazovetsky, Y. On the Use of Remote Sensing Data to Study the Geological Structure and Forecast Mineral Resources of the Shu-Ile Suture. *Geol. Geogr. Glob. Energy* 2024. [CrossRef]
17. Tleubergenova, A.; Umirova, G.; Maussymbayeva, A.; Portnov, V. Comprehensive Analysis of Magnetic and Gravity Data Based on Volumetric Gravity-Magnetic Modeling along the Geotraverse in the Shu-Sarysu Sedimentary Basin. *Visnyk Taras Shevchenko Natl. Univ. Kyiv. Geol.* **2023**, *3*, 31–38. [CrossRef]
18. Amangeldy Gas LLP. Official Website. Available online: https://amangeldygas.kz/ (accessed on 10 May 2025).
19. Akchulakov, U.; Zholtaev, G.G.; Kuandykov, B.M.; Iskaziev, K. *Atlas of Oil and Gas Bearing and Prospective Sedimentary Basins of the Republic of Kazakhstan*; KazMunayGas: Astana, Kazakhstan, 2014; p. 97.
20. Dikenshteyn, G.K.; Maksimov, S.P.; Semenovich, V.V. *Oil-Gas Provinces of the USSR*; Nedra: Moscow, Russia, 1983; p. 272.
21. Kuchapin, A.V. On the Prospects of Oil and Gas Potential of the Meso-Cenozoic Deposits of the Chu Depression. *Geol. Nefti* 1957, 1–7.

22. Ulmishek, G.F.; Masters, C.D. *Estimated Petroleum Resources in the Former Soviet Union*; U.S. Geological Survey: Reston, VA, USA, 1993. [CrossRef]
23. Zholtaev, G.Z. Oil and Gas Basins of Kazakhstan from the Perspective of Plate Tectonics. In *Deep Structure and Metallogeny of Kazakhstan*; Nauka: Almaty, Kazakhstan, 1997; pp. 71–79.
24. Maemer, M.S.; Ismailova, G.A. Oil and Gas Potential of Shu-Sarysu Depression. *Vestn. Kazn.* **2012**, *4*, 31–38.
25. Korobkin, V.V.; Tulemissova, Z.S. Estimation of the Forecast Hydrocarbon Resource Potential of the Shu-Sarysu, Ili and Pre-Balkhash Sedimentary Basins of Southern Kazakhstan. In Proceedings of the International Scientific and Practical Conference "Condition and Prospects for the Development of Mature Fields", Aktau, Kazakhstan, 16–17 May 2019.
26. Paragulgov, T.K.; Paragulgov, K.K. Classifying of East Kazakhstan Sedimentary Basins and Their Oil and Gas Potential. In Proceedings of the 72nd EAGE Conference & Exhibition, Barcelona, Spain, 14–17 June 2010. [CrossRef]
27. Magoon, L.; Dow, W. The Petroleum System: From Source to Trap. *AAPG Mem.* **1994**, *60*, 25–49. [CrossRef]
28. Daukeev, S.Z.; Votsalevskiy, E.S.; Uzhkenov, B.S. *Deep Structure and Mineral Resources of Kazakhstan*; Oil and Gas: Almaty, Kazakhstan, 2002; p. 248.
29. Windley, B.F.; Alexeiev, D.; Xiao, W.; Kroner, A.; Badarch, G. Tectonic Models for Accretion of the Central Asian Orogenic Belt. *J. Geol. Soc.* **2007**, *164*, 31–47. [CrossRef]
30. Li, A.B.; Mailibaev, M.M.; Tukenov, N.T. *Chu Depression. Geology of the USSR*; Nedra: Moscow, Russia, 1971; p. 100.
31. Bakirov, A.B. Stratigraphy of the Upper Paleozoic Deposits of the Chu Depression and Maly Karatau. Stratigraphy of the Devonian, Carboniferous, and Permian of Kazakhstan. *Nauka* **1974**, *2*, 178–183.
32. Mustafaev, Z.S.; Kozykeeva, A.T.; Shugayyp, U.; Abdeshev, K.; Tursynbayev, N. Analysis and Assessment of Variability of the Hydrological Regime of the Rivers of the Sarysu Basin in Spatial and Temporal Aspects. *Geogr. I Vodn. Resur.* **2024**, *4*, 54–66. [CrossRef]
33. Bekzhanov, G.R.; Koshkin, V.Y.; Nikitchenko, L.I.; Skrinnik, G.R. *Geological Structure of Kazakhstan*; AMR RK: Almaty, Kazakhstan, 2000; p. 396.
34. Korobkin, V.V.; Tulemissova, Z.S. Specific Features of the Geological Structure and Geodynamic Setting of the Shu-Sarysu Sedimentary Basin in the Late Paleozoic. Influence of External Fields on Seismic Regime and Monitoring of Their Manifestations. In Proceedings of the International Jubilee Scientific Conference, Bishkek, Kyrgyzstan, 3–7 July 2018.
35. Baibatsha, A.; Vyazovetsky, Y.V.; Kembayev, M.; Rais, S.; Koishina, G.M.; Talgatbek, A.N. Geology and Metallogeny of Shu-Ile Ore Zone Intrusive Complexes (Kazakhstan). *Preprints* **2024**, 2024041120. [CrossRef]
36. Korobkin, V.V.; Tulemissova, Z.S. Deep Structure and Geodynamic Conditions of Sedimentary Basin Formation in Southern Kazakhstan (Shu-Sarysu, Pre-Balkhash, Ili). *Geol. Okhr. Nedr KazGeo* **2018**, *3*, 24–34.
37. Shakhov, R.A.; Rzhannikova, L.N. Stratigraphy of the Upper Devonian of the Chu Depression. In *Stratigraphy of the Devonian, Carboniferous, and Permian of Kazakhstan*; Nauka: Alma-Ata, Kazakhstan, 1974; p. 58.
38. Cook, H.E.; Zhemchuzhnikov, V.G.; Zempolich, W.G.; Makarov, V.I.; Sadybekov, B.; Osmonbetov, K. Devonian and Carboniferous Carbonate Platform Facies in the Bolshoi Karatau, Southern Kazakhstan: Outcrop Analogs for Coeval Carbonate Oil and Gas Fields in the North Caspian Basin. In *Oil and Gas of the Greater Caspian Area*; Yilmaz, P.O., Isaksen, G.H., Eds.; AAPG Studies in Geology 55; American Association of Petroleum Geologists: Tulsa, OK, USA, 2007; pp. 159–163. [CrossRef]
39. Wang, Y.; Lin, C.; Sun, Y.; Liu, J.; Li, H.; He, H.; Wang, Q.; Ji, M.; Zhang, M.; Zhao, B.; et al. Depositional Sequences and Microfacies of Early Carboniferous Strata in the Marsel Block of the Chu-Sarysu Basin, Southern Kazakhstan. *Carbonates Evaporites* **2020**, *35*, 43. [CrossRef]
40. Zhumagulov, A.S.; Ismailova, J.A. Stratigraphy and Lithology of the Paleozoic Deposits in the Tasbulak Graben, Shu-Sarysu Basin. *Neft i Gaz* **2023**, *5*, 6–16. [CrossRef]
41. Korobkin, V.V.; Samatov, I.B.; Tulemisova, Z.S. Study of the Material Composition of the Rocks of the Coal-Permian Section of the Southwestern Part of the Shu-Sarysu Oil and Gas Basin. In Proceedings of the International Jubilee Conference Dedicated to the 40th Anniversary of the Research Station RAS in Bishkek City "Influence of External Fields on Seismic Regime and Monitoring of Their Manifestations", Bishkek, Kyrgyzstan, 3–7 July 2018.
42. Pang, X.; Li, Q.; Chen, J.; Li, M.; Pang, H. Recovery method of original TOC and its application in source rocks at high mature–over mature stage in deep petroliferous basins. *J. Palaeogeogr.* **2014**, *16*, 769–789.
43. Zhao, Z.; Pang, X.; Li, Q.; Hu, T.; Wang, K.; Li, W.; Guo, K.; Li, J.; Shao, X. Depositional Environment and Geochemical Characteristics of the Early Carboniferous Source Rocks in the Marsel Area, Shu-Sarysu Basin, Southern Kazakhstan. *Mar. Pet. Geol.* **2017**, *81*, 134–148. [CrossRef]
44. Tulemissova, Z.S.; Korobkin, V.V.; Buslov, M.M. Correlation of the Stratigraphic Section with the Assessment of Forecasted Hydrocarbon Resources of Sedimentary Basins in Southern Kazakhstan (Shu-Sarysu, Ili and Pribalkhash). *Vestn. KBTU* **2019**, *4*, 177–185.
45. Madenova, A.A.; Abdrakhmanov, M.K.; Uzbekgaliev, R.H. Lithological Features of Chu-Sarysu Depression's Section Taking into Account the Differentiation of the Geological Structure. *Vestn. Kazn.* **2018**, *2*, 40–45.

46. Baratov, R.T.; Seitmuratova, E.Y.; Murtazin, E.Z. Lithium Concentrations in Saline Brines of the Shu–Sarysu Depression. *Appl. Sci.* **2024**, *14*, 5351. [CrossRef]
47. Bykadorov, V.A.; Fedorenko, O.A.; Miletenko, N.V. *Atlas of Lithological-Paleogeographic, Structural, Palinspastic and Geoecological Maps of Central Eurasia*; YUGGEO: Almaty, Kazakhstan, 2002.
48. Dickenstein, G.H.; Sinitsin, F.E.; Sokolova, E.A. Geological Structure and Oil and Gas Possibilities of the West-Chuesk Depression. *OilGasGeo* **1963**, *5*, 23–30.
49. Li, A.B.; Vlasov, V.I.; Paragul'gov, K.K. *Tectonic Development and Oil and Gas Potential of the Shu-Sarysu Depression*; Nauka: Moscow, Russia, 1982; p. 157.
50. Ulykpanova, M.M.; Auezova, Z.; Ramazanova, N.; Mussabaeva, M.; Zhanguzhina, A.A. Application of Remote-Sensing Data in Geochemical Studies of Soils of the Yertis River Basin Within East Kazakhstan. *Quaest. Geogr.* **2024**, *43*, 157–164. [CrossRef]
51. Veynmar, A.B.; Kuzmin, A.V.; Vorontsova, T.N. Geological Events in Kazakhstan at the Frasnian–Famennian Boundary and Thteir Importance among Global Events of That Time. *Bull. Soc. Nat. Explor. Geol. Sect.* **1997**, *72*, 35–46.
52. Kurchavov, A.M.; Grankin, M.S.; Malchenko, E.G.; Zhukovsky, V.I.; Mazurov, A.K.; Khamzin, B.S. Zonation, Segmentation and Paleogeodynamics of the Devonian Volcanic Belt of Central Kazakhstan. *Geotektonika* **2000**, *4*, 32–43.
53. Patalakha, E.I.; Abdulin, A.A.; Apollonov, M.K.; Korobkin, V.V.; Lukienko, A.I. Chu-Ili Ore Belt. In *Geology of the Chu-Ili Region*; Nauka: Alma-Ata, Kazakhstan, 1980; p. 504.
54. Ryazantsev, A.V.; Tolmacheva, T.Y.; Degtyarev, K.E.; Kotov, A.B.; Sal'nikova, E.B.; Anisimova, I.V.; Yakovleva, S.Z. Geochronological and Biostratigraphic Justification of the Age of Ophiolites of the Dzhalaïr-Naiman Zone, Kazakhstan. *GEOS* **2008**, *2*, 214–219.
55. Abetov, A.E.; Uzbekov, A.N. Deep Structure of Central Kazakhstan. *Vestn. Kazn.* **2019**, 28–34.
56. Zhang, M.; Lin, C.; Sun, Y.; Liu, J.; Li, H.; Wang, Q.; Wang, Y. Sequence Framework, Depositional Evolution and Controlling Processes, the Early Carboniferous Carbonate System, Shu-Sarysu Basin, Southern Kazakhstan. *Mar. Pet. Geol.* **2020**, *50*, 1585–1603. [CrossRef]
57. Abdulin, A.A.; Patalakha, E.I. *Geodynamics of the Earth's Crust of Kazakhstan*; Nauka: Alma-Ata, Kazakhstan, 1999; p. 176.
58. Ageev, B.D. On the History of Formation of Middle Paleozoic Evaporites in the Chu-Sarysu Depression in Connection with Oil and Gas Prospecting in Southern Kazakhstan. *Nauka* **1982**, 89–97.
59. Apollonov, M.K. Geodynamic Evolution of Kazakhstan in the Early Paleozoic (from the Perspective of Classical Plate Tectonics). *Geodyn. Miner. Genes. Kazakhstan* **2000**, *1*, 46–63.
60. Buslov, M.M. Tectonics and Geodynamics of the Central Asian Orogenic Belt: Role of Late Paleozoic Large-Amplitude Strike-Slip Faults. *Geol. Geophys.* **2011**, *52*, 66–90.
61. Galitsky, V.V. Tectonics of the Karatau Ridge (Southern Kazakhstan). In *Tectonics and Dynamometamorphism of the Paleozoic of Kazakhstan*; Nauka: Alma-Ata, Kazakhstan, 1967; Volume 19, pp. 3–47.
62. Didenko, A.N.; Mossakovsky, A.A.; Pechersky, D.M.; Ruzhentsev, S.V.; Samygin, S.G.; Kheraskova, T.N. Geodynamics of Paleozoic Oceans of Central Asia. *Geol. Geophys.* **1994**, *35*, 59–75.
63. Dobretsov, N.L. Evolution of the Structures of the Urals, Kazakhstan, Tien Shan and the Altai-Sayan Region in the Ural-Mongolian Fold Belt (Paleoasian Ocean). *Geol. Geophys.* **2003**, *44*, 5–27.
64. Dobretsov, N.L.; Buslov, M.M. Late Cambrian–Ordovician Tectonics and Geodynamics of Central Asia. *Geol. Geophys.* **2007**, *48*, 93–108. [CrossRef]
65. Ermolov, P.V. Geodynamics of Kazakhstan. In Proceedings of the International Scientific and Practical Conference "Geological Science and Industrial Development of the Republic of Kazakhstan", Dedicated to the 70th Anniversary of the Institute of Geological Sciences Named after K.I. Satpayev, Almaty, Kazakhstan, 12 April 2010.
66. Korobkin, V.V.; Buslov, M.M. Tectonics and Geodynamics of the Kazakhstan Paleozoid. In *Earth Sciences in Kazakhstan*; KazGEO: Almaty, Kazakhstan, 2016; p. 498.
67. Korobkin, V.V.; Smirnov, A.V. Paleozoic Tectonics and Geodynamics of Volcanic Arcs of Northern Kazakhstan. *Geol. Geophys.* **2006**, *4*, 462–474.
68. Kurishbaev, A.; Amanzholova, R.; Adenova, D.; Sagin, J.; Burlibayeva, D.; Sarsekova, D.; Alikhanov, K.D.; Serikkanov, A.S.; King, R. Comparative Assessment of the Mountainous River Basin in Kyrgyz-Kazakh Region of Central Asia with River Basins in Australia, Canada and USA. *Grassroots J. Nat. Resour.* **2024**, *7*, 79–96. [CrossRef]
69. Mailibaev, M.M. *Tectonic Features of the Formation of the Middle and Upper Paleozoic of the Chu Depression in Relation to Oil and Gas Prospects*; Nauka: Alma-Ata, Kazakhstan, 1968; p. 140.
70. Allen, M.B.; Alsop, G.I.; Zhemchuzhnikov, V.G. Dome and Basin Refolding and Transpressive Inversion along the Karatau Fault System, Southern Kazakhstan. *J. Geol. Soc.* **2001**, *158*, 83–95. [CrossRef]
71. Korobkin, V.V.; Buslov, M.M. Tectonics and Geodynamics of the Western Central Asian Fold Belt (Kazakhstan Paleozoides). *Russ. Geol. Geophys.* **2011**, *52*, 1600–1618. [CrossRef]

72. Kroner, A.; Windley, B.F.; Badarch, G.; Tomurtogoo, O.; Hegner, E.; Jahn, B.M.; Gruschka, S.; Khain, E.V.; Demoux, A.; Wingate, M.T.D. Accretionary Growth and Crust Formation in the Central Asian Orogenic Belt and Comparison with the Arabian-Nubian Shield. In *4-D Framework of Continental Crust*; Hatcher, R.D., Carlson, M.P., McBride, J.H., Martínez Catalán, J.R., Eds.; Geological Society of America Memoirs; Geological Society of America: Boulder, CO, USA, 2007; pp. 181–209. [CrossRef]
73. Li, P.; Sun, M.; Rosenbaum, G.; Yuan, C.; Safonova, I.; Cai, K.; Jiang, Y.; Zhang, Y. Geometry, Kinematics and Tectonic Models of the Kazakhstan Orocline: Central Asian Orogenic Belt. *J. Asian Earth Sci.* **2018**, *153*, 42–56. [CrossRef]
74. Sengor, A.M.C.; Natal'in, B.A.; Burtman, V.S. Evolution of the Altaid Tectonic Collage and Palaeozoic Crustal Growth in Eurasia. *Nature* **1993**, *364*, 299–307. [CrossRef]
75. Tulemissova, Z.S.; Buslov, M.M.; Bekmukhametova, Z.A. Geodynamic Conditions of Formation of Sedimentary Basins of South Kazakhstan (Shu-Sarysu, Pre-Balkhash, Ili). Petrology of Magmatic and Metamorphic Complexes. In Proceedings of the IOP Conference Series: Earth and Environmental Science, Tomsk, Russia, 27–30 November 2019. [CrossRef]
76. Alekseev, V.P.; Glumakov, P.V.; Kornienko, G.E.; Mamadjanov, E.A.; Obukhov, A.N.; Orudzheva, D.S.; Tabachnikova, E.K. *Tectonics, Formations, and Oil and Gas Potential of Intermontane Depressions: Central Asia and Kazakhstan*; Zolotov, A.N., Krylov, N.A., Eds.; Nauka: Moscow, Russia, 1988; p. 128.
77. Bykadorov, V.A.; Bush, V.A.; Fedorenko, O.A.; Filatova, N.I.; Zhabin, S.V.; Kruglikov, N.M. Ordovician–Permian Paleogeography of Central Eurasia: Development of Palaeozoic Petroleum-Bearing Basins. *J. Pet. Geol.* **2003**, *26*, 325–350. [CrossRef]
78. De Pelsmaeker, E.; Glorie, S.; Buslov, M.M.; Verchoots, M.; Leys, C.; Van den Haute, P. Late-Palaeozoic Emplacement and Meso-Cenozoic Reactivation of the Southern Kazakhstan Granitoid Basement. *Tectonophysics* **2015**, *662*, 416–433. [CrossRef]
79. Ren, R.; Liu, B.; Han, B.-F.; Guan, S.-W. Early-Middle Devonian Adakitic Magmatism Generated by Slab Retreat in Southern West Junggar, NW China: Implications for Tectonic Correlation with Central and East Kazakhstan. *Int. Geol. Rev.* **2022**, *65*, 2315–2331. [CrossRef]
80. Tikhomirov, V.G. Inherited Trends in the Development of the Palaeozoic Structures of the Sarysu-Teniz Uplift (Central Kazakhstan). *Int. Geol. Rev.* **1959**, *1*, 41–50. [CrossRef]
81. Tulemissova, Z.S.; Korobkin, V.V. Features of the Geodynamic Evolution of the Main Oil and Gas Basins of Kazakhstan in the Palaeozoic. *Int. J. Eng. Res. Technol.* **2020**, *13*, 1045–1056. [CrossRef]
82. Yurina, A.L.; Zavrazhnov, V.N.; Chechik, N.L. New Data about the Age of Devonian Volcanic Piles of the Southern Part of the Sarysu-Teniz Divide (Central Kazakhstan). *Vestn. Mosk. Univ., Ser. Geol.* **1982**, *1*, 33–37.
83. Fazylov, E.M.; Prikhodko, D.E.; Mussina, E.S. Facial-Paleogeographic Conditions of Accumulation of the Late Devonian Saliferous Strata of the Syrdarya Sedimentary Basin. *Geol. Pol. Iskop. Kazakhstana* **2017**, *5*, 62–70.
84. Kurmanbayev, R.; Shmanov, A.; Zhaksylyk, E.; Duisembayev, A. Tectonic Zoning and Hydrocarbon Prospectivity of the Chu–Sarysu Basin. *Geol. Subsurf. Resour. Kazakhstan* **2022**, *4*, 45–58.
85. Torsvik, T.H.; Cocks, L.R.M. *Earth History and Palaeogeography*; Cambridge University Press: Cambridge, UK, 2017; p. 317. [CrossRef]
86. Duysembekov, B.; Issagulov, M.; Kozhakhmetov, N. Geological Evolution and Structural Features of Paleozoic Basins in Central Kazakhstan. *Bull. Kazakh Nat. Technol. Univ.* **2020**, *6*, 12–25.
87. Zonenshain, L.P.; Kuzmin, M.I.; Natapov, L.M. *Geology of the USSR: A Plate-Tectonic Synthesis*; American Geophysical Union: Washington, DC, USA, 1990; p. 242. [CrossRef]
88. Alekseev, D.V.; Bykadorov, V.A.; Volozh, Y.A.; Sapozhnikov, R.B. Kinematic Analysis of the Jurassic Grabens of South Turgay and the Role of the Mesozoic Stage in the History of the Karatau-Talaso-Fergana Shear Zone (Southern Kazakhstan and Tien Shan). *Geotektonika* **2017**, *2*, 3–20.
89. Zholtaev, G.Z.; Kuandykov, B.M. Geodynamic Model of the Structure of Southern Eurasia. *Neft i Gaz* **1999**, *2*, 62–74.
90. Bigeldiyev, A.; Batu, A.; Berdibekov, A.; Zhumagulov, A.; Narimanov, Y. Dynamic modeling of the gas discharge of a mine in the Karaganda coal basin under high uncertainty using a multiple realization approach. In Proceedings of the SPE Russian Petroleum Technology Conference, Moscow, Russia, 12–15 October 2021. [CrossRef]
91. Li, Q.; Pang, X.; Tang, L.; Li, W.; Zhang, K.; Zheng, T.; Zhang, X. Insights into the Origin of Natural Gas Reservoirs in the Devonian System of the Marsel Block, Kazakhstan. *J. Earth Sci.* **2019**, *30*, 893–907. [CrossRef]
92. Li, Q.; Pang, X.; Li, B.; Zhao, Z.; Shao, X.; Zhang, X.; Wang, Y.; Li, W. Discrimination of Effective Source Rocks and Evaluation of the Hydrocarbon Resource Potential in Marsel, Kazakhstan. *J. Pet. Sci. Eng.* **2018**, *160*, 194–206. [CrossRef]
93. Wu, X.; Li, N.; Zhou, L.; Yu, D.; Cha, Y. Distribution and Origin of Molecular Nitrogen in Natural Gas of Kokpansor Depression, Chu-Sarysu Basin. *J. China Univ. Pet.* **2015**, *39*, 35–41. [CrossRef]
94. Huang, H.; Xiang, K.; Wang, Y.; Zhang, S.; Li, B.; Yang, Y.; Li, J. Application of Matching Pursuit Method for Detection of Fluid in Carbonate Rock: A Case Study from Chu-Sarysu Basin in Kazakhstan. *Shiyou Xuebao/Acta Pet. Sin.* **2015**, *36*, 184–193. [CrossRef]
95. Seithaziyev, Y.S. Geochemical Studies of Condensate, Gas and Core Samples Derived from Gas-Condensate Fields in the Moynkum Sag (Kazakhstan). News of the National Academy of Sciences of the Republic of Kazakhstan. *Ser. Geol. Technol. Sci.* **2023**, *3*, 242–261. [CrossRef]

96. Xiongqi, Z.; Handong, H.; Changsong, L.; Xiaomin, Z.; Yong, L.; Jianfa, C.; Yongshang, K.; Guoping, B.; Guangda, W.; Xinsong, W.; et al. Formation, distribution, exploration, and resource/reserve assessment of superimposed continuous gas field in Marsel exploration area, Kazakhstan. *Acta Pet. Sin.* **2014**, *35*, 1012–1056. [CrossRef]
97. Tulemissova, Z.S.; Buslov, M.M.; Bekmukhametova, Z.A. Data of Studying the Content of Organic Matter in Deposits of the Stone-Perm Separation of the Southwestern Part of the Shu-Sarysu Basin. Petrology of Magmatic and Metamorphic Complexes. In Proceedings of the IOP Conference Series: Earth and Environmental Science, Tomsk, Russia, 27–30 November 2018. [CrossRef]
98. Box, S.E.; Syusyura, B.; Hayes, T.S.; Taylor, C.D.; Zientek, M.L.; Hitzman, M.W.; Seltmann, R.; Chechetkin, V.; Dolgopolova, A.; Cossette, P.M.; et al. *Sandstone Copper Assessment of the Chu-Sarysu Basin, Central Kazakhstan*; U.S. Geological Survey Scientific Investigations Report 2010-5090-E; U.S. Geological Survey: Reston, VA, USA, 2012. [CrossRef]
99. Zhang, K.; Pang, X.; Zhao, Z.; Shao, X.; Zhang, X.; Li, W.; Wang, K. Pore Structure and Fractal Analysis of Early Carboniferous Carbonate Reservoirs in the Marsel Area, Shu-Sarysu Basin. *Mar. Pet. Geol.* **2018**, *93*, 451–467. [CrossRef]
100. Minskiy, N.A.; Sokolova, V.A. Secondary Mineralization and Oil Potential of Early Carboniferous Rocks in Chu-Sarysu Basin in Relation to Tectonic Activity. *Int. Geol. Rev.* **1974**, *16*, 741–748. [CrossRef]
101. Bykadorov, V.A.; Volozh, V.A.; Antipov, M.P. Salt-Dome Structures of the Shu-Sarysu Basin (Central Kazakhstan). *Lithosphere* **2015**, *4*, 14–23. Available online: https://doaj.org/article/4d85c9f142414b20b1e8fe5974188bef (accessed on 10 May 2025).
102. Kopobayeva, A.; Baidauletova, I.; Amangeldikyzy, A.; Askarova, N. Trace Elements Distribution in the K7 Seam of the Karaganda Coal Basin, Kazakhstan. *Geosciences* **2024**, *14*, 143. [CrossRef]
103. Paragulgov, K.K.; Li, A.B.; Filip'ev, G.P.; Shlygin, D.A.; Shlygina, T.M. Nature of the Sarysu Salt Domes. *Vestn. Akad. Nauk KazSSR* **1983**, *6*, 53–59.
104. Sharapatov, A.; Assirbek, N.; Abdyrov, M.; Saduov, A. Evaluation of Filtration Properties of Ore-Bearing Rocks According to Electrical Logging Methods (Shu-Sarysu Uranium Province, Kazakhstan). *Univ. Enbekteri* **2024**, *3*. [CrossRef]
105. Bykadorov, V.A.; Volozh, V.A.; Antipov, M.P. Age and Tectonic Position of Salt Dome Structures of the Shu-Sarysu Basin (Central Kazakhstan). *Geol. MOIP* **2014**, *6*, 3–11.
106. Kunin, N.Y. Tectonic Structure and Prospects of Oil and Gas Potential in the Southwestern Part of the Chu-Sarysu Depression. *Izv. Akad. Nauk. KazSSR Ser. Geol.* **1961**, *43*.
107. Kunin, N.Y. *Tectonics of the Middle Syrdarya and Chu-Sarysu Depressions Based on Geophysical Data*; Nedra: Moscow, Russia, 1968; p. 264.
108. Li, A.B. *Tectonics and Prospects for Oil and Gas Potential of Southern Kazakhstan*; Nauka: Alma-Ata, Kazakhstan, 1975; p. 220.
109. Abetov, A.E.; Zhumagulov, A.S. Geochemical and Hydrogeological Indicators of Oil and Gas Potential of the Middle-Upper Paleozoic Deposits of the Shu-Sarysu Depression. Actual Tasks of Oil and Gas and Ore Geophysics. In Proceedings of the Satpayev Readings Conference, Almaty, Kazakhstan, 12 April 2021.
110. Nevsky, G.K. Tectonic Prerequisites for Search for Oil and Gas in Palaeozoic Deposits of the Chu-Sarysui Depression. *OilGasGeo* **1962**, 14–20.
111. Korobkin, V.V. Tectonic Zoning and Structural Styles of the Palaeozoids of Kazakhstan. *Izv. Tomsk. Polytechnol. Univ.* **2011**, *319*, 71–77.
112. Tulemissova, Z.S. Comparative Characteristics and Conditions of Formation of Hydrocarbons Sediment Traps in the West Siberian, Shu-Sarysu and Caspian Basins. *News NAS RK Ser. Geol. Technol. Sci.* **2017**, *2*, 56–62.
113. Sinitsyn, F.E.; Karpov, V.I.; Filip'ev, G.P. Significance of Migration in Gas Deposit Formation in the Western Part of Chu-Sarysu Syneclise. *Russ. Oil Gas Geol.* **1978**, *6*, 37–40.
114. Adenova, D.; Sarsekova, D.; Absametov, M.; Murtazin, Y. The Study of Groundwater in the Zhambyl Region, Southern Kazakhstan, to Improve Sustainability. *Sustainability* **2024**, *16*, 4597. [CrossRef]
115. Cook, H.E.; Zhemchuzhnikov, V.G.; Zempolich, W.G.; Lehmann, P.J.; Alexeiev, D.V.; Zhaimina, V.Y.; Zorin, A.Y. Devonian and Carboniferous Carbonate Platform Facies in the Bolshoi Karatau, Southern Kazakhstan: Outcrop Analogs for Coeval Carbonate Oil and Gas Fields in the North Caspian Basin, Western Kazakhstan. *SEPM Spec. Publ.* **2002**, *74*, 81–122. [CrossRef]
116. Beznosov, N.V.; Gurari, F.G.; Ilyin, V.D.; Mesezhnikov, M.S.; Lipatova, V.V. *Reference Book on the Stratigraphy of Petroleum Provinces of the USSR*; Nedra: Moscow, Russia, 1987; p. 336.
117. Filippova, I.B.; Bush, V.A.; Didenko, A.N. Middle Paleozoic subduction belts: The leading factor in the formation of the Central Asian fold-and-thrust belt. *Russ. J. Earth Sci.* **2001**, *3*, 405–426. [CrossRef]
118. Amirgali, A.M.; Umirova, G.K.; Akhmetzhanov, A.Z. Gas and Oil-Bearing Potential of Middle–Upper Paleozoic Deposits of the Kokpansor Depression Based on 3D Seismic and Deep Drilling Data. Innovative Technologies—Key to the Successful Solution of Fundamental and Applied Problems in the Ore and Oil and Gas Sectors of the Economy of the Republic of Kazakhstan. In Proceedings of the Satpayev Readings Conference, Almaty, Kazakhstan, 10–11 April 2019.
119. Barbosa, G.S.; Garcia, G.G.; Pena dos Reis, R.P.B.; Garcia, A.J.V.; Barberes, G.d.A. Analysis of the Efficiency of Petroleum Systems in Fluvial Environments in the Rift Context of the South and North Atlantic: Brazil and Portugal. *Geosciences* **2023**, *13*, 239. [CrossRef]

120. Perrodon, A.; Masse, P. Subsidence, Sedimentation and Petroleum Systems. *J. Pet. Geol.* **1984**, *7*, 5–25. [CrossRef]
121. Al Hajeri, M.M.; Al Saeed, M.; Derks, J.; Fuchs, T.; Hantschel, T.; Kauerauf, A.; Neumaier, M.; Schenk, O.; Swientek, O.; Tessen, N.; et al. Basin and Petroleum System Modeling: Bridging Geologic History with Hydrocarbon Prospectivity. *Oilfield Rev.* **2009**, *21*, 14–29. Available online: https://www.researchgate.net/publication/284661928 (accessed on 1 June 2025).
122. Carpentier, C. Middle Clays as indicators of paleoclimate and source rocks in the Chu-Sarysu Basin (Kazakhstan). *Kazakhstan J. Oil Gas Ind.* **2023**, *1*, 21–35. [CrossRef]

Disclaimer/Publisher's Note: The statements, opinions and data contained in all publications are solely those of the individual author(s) and contributor(s) and not of MDPI and/or the editor(s). MDPI and/or the editor(s) disclaim responsibility for any injury to people or property resulting from any ideas, methods, instructions or products referred to in the content.